2015

Na+/K+ Pump and Cl--coupled Na+ and K+ co-transporters in Mouse Embryonic Fibroblasts lacking the Tuberous Sclerosis Complex TSC1 and TSC2 genes.

Jasser Ali S. Alzhrani
Wright State University

Na^+/K^+ Pump and Cl^--coupled Na^+ and K^+ co-transporters in Mouse Embryonic Fibroblasts lacking the Tuberous Sclerosis Complex TSC1 and TSC2 genes.

A thesis submitted in partial fulfillment of the requirements for the degree of Master of Science

By

JASSER ALI S ALZHRANI

Bachelor of Pharmacy, King Khalid University, Saudi Arabia, 2008

2015

Wright State University

WRIGHT STATE UNIVERSITY

GRADUATE SCHOOL

July 31, 2015

I HEREBY RECOMMEND THAT THESIS PREPARED UNDER MY SUPERVISION BY Jasser Ali S Alzhrani ENTITLED Na^+/K^+ Pump and Cl^--coupled Na^+ and K^+ co-transporters in Mouse Embryonic Fibroblasts lacking the Tuberous Sclerosis Complex TSC1 and TSC2 genes. BE ACCEPTED IN PARTIAL FULLFILMENT OF THE REQUIREMENTS FOR THE DEGREE OF Master of Science.

_____

Norma Adragna, Ph.D.
Thesis Advisor

_____

Jeffrey B. Travers, M.D., Ph.D.
Chair, Department of
Pharmacology and Toxicology

Thesis Committee

_____

Norma Adragna, Ph.D.

_____

Peter Lauf, M.D.

_____

Jeffrey B. Travers, M.D., Ph.D.

_____

Robert E. W. Fyffe, Ph.D.
Vice President for Research and
Dean of the Graduate School

Abstract

Alzhrani, Jasser Ali. M.S. Department of Pharmacology and Toxicology, Wright State University, 2015. Na^+/K^+ Pump and Cl^--coupled Na^+ and K^+ cotransporters in Mouse Embryonic Fibroblasts lacking the Tuberous Sclerosis Complex 1 (TSC1) and Tuberous Sclerosis Complex 2 (TSC2) genes.

The tuberous sclerosis complex 1 and 2 (TSC1 and TSC2) genes and their products hamartin and tuberin, respectively, are involved in several regulatory cellular mechanisms, including the mTOR pathway that is important for proliferation, cell migration, and protein synthesis. In addition, it has been suggested that this pathway plays a role in regulating Na^+-K^+-$2Cl^-$ and K^+-Cl^- cotransporters (NKCC and KCC, respectively) [41, 42, 43]. Therefore, the TSC1 and TSC2 genes are expected to play a significant role in regulating cell volume, and K^+ and Cl^- homeostasis. This study tests the hypothesis that the TSC1 and TSC2 genes, which control cell processes through the mTOR pathway, are important for the function of the Na^+/K^+ pump (NKP), Na^+,K^+,$2Cl^-$ and K^+,$2Cl^-$ cotransporters (KCC and KCC, respectively) and for the maintenance of intracellular K^+ (K_i) content in mouse embryonic fibroblasts (MEF) cells. The cellular models are wild type (WT) and knockouts (KO) of the TSC1 or TSC2 genes, TSC1-KO and TSC2-KO, respectively. K^+ homeostasis was assessed through the activities of NKP, NKCC and KCC determined by rubidium (Rb^+, a K^+ congener) influx and K_i content in the presence and absence of the NKP-inhibitor ouabain, the NKCC-inhibitor bumetanide and by Cl^--dependent Rb^+ influx via KCC. Optimal ouabain and bumetanide concentrations were obtained from the dose-response curves of Rb^+ influx and K_i content inhibition toward these compounds. In support of the hypothesis, the main findings

indicate that absence of the TSC1, and especially, the TSC2 gene, which are associated with depression of the mTOR pathway [4, 5, 8], leads to accelerated cell proliferation and migration, and abnormal activities of all the transporters tested revealing the importance of the TSC1 and TSC2 gene products, hamartin and tuberin, respectively, in cellular K^+ homeostasis in MEF cells. Moreover, abnormalities in ion transport of TSC2-KO cells is commensurate with the pathological manifestation and incidence of tuberous sclerosis complex in the human population. These findings also uncover potential targets for more efficient therapy.

Table of contents

List of figures

List of tables

1. Introduction

Most cellular functions crucially depend on cell volume. In addition, the structure and function of molecules, and especially of macromolecules such as enzymes, are altered by hydration [1]. The cellular membrane is highly permeable to water and is responsive to changes in the intracellular or extracellular osmolality. The cell membrane's permeability to Na^+, K^+ and Cl^- ions is orders of magnitude lower than that to water Therefore, in order to maintain a stable cell volume, all cells express various transport proteins for Na^+, K^+ and Cl^- across the cell membrane [1, 2].

A brief overview of cell volume regulatory mechanisms will be given here. When cells are exposed to several osmolalities such as hypotonic, isotonic or hypertonic, they may undergo volume changes and become swollen, normal or shrunken, respectively. Swollen cells may undergo regulatory volume decrease (RVD) by releasing ions, particularly activation of volume-sensitive Cl^- and K^+ channels and K^+- Cl^- cotransport (KCC). Shrunken cell may undergo regulatory volume increase (RVI) by taking up ions, particularly through the Na^+/H^+ exchanger, Na^+- K^+- $2Cl^-$ co-transporter (NKCC), and non-selective cation channels [1, 2] (Fig. 1).

We explore in this study the characteristics of the Na^+/K^+ Pump and Cl^--coupled Na^+ and K^+ co-transporters (NKCC and KCC) in mouse embryonic fibroblasts (MEFs) lacking the tuberous sclerosis complex-1 (TSC1) and -2 (TSC2) genes. The cell models used are wild type (WT), TSC1-KO, and TSC2-KO. Before providing a more detailed

description of the study, a brief introduction about TSC 1 and 2, the mammalian target of rapamycin (mTOR) complex 1 and 2, NKP, NKCC, and KCC will be presented.

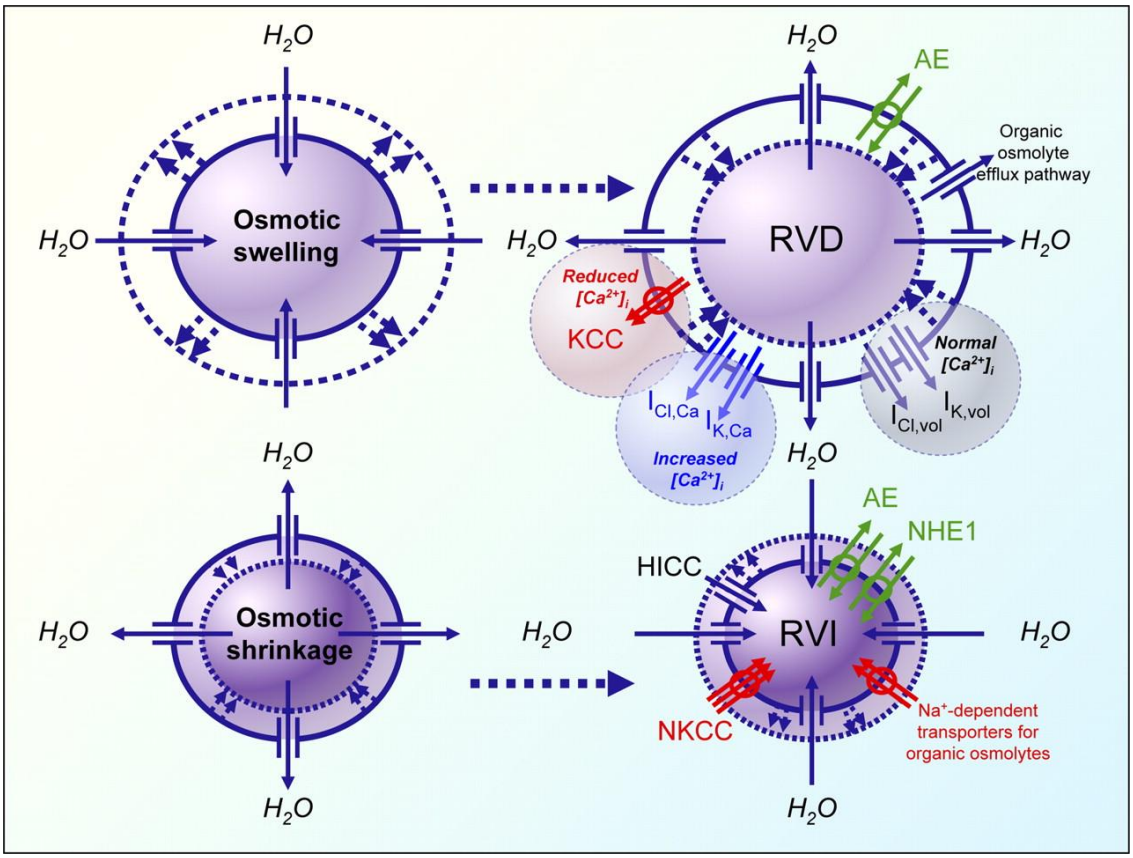

Figure 1 - Effectors involved in regulatory volume decrease (RVD) and regulatory volume increase (RVI) [32]. The main effectors in RVI in most cell types are Na^+/H^+ exchangers (NHEs), the Na^+-K^+-$2Cl^-$Cotransporters (NKCCs), anion exchange (AE), hypertonicity-induced cation channels (HICCs), and Na-dependent transporters for organic osmolytes. However, the main effectors in RVD are swelling-activated Cl^- channels ($I_{cl,vol}$), swelling-activated K^+ channels ($I_{k,vol}$), anion exchange (AE), the K^+-Cl^- cotransporters (KCCs), and organic osmolyte efflux pathways.

1.1. Tuberous sclerosis complex 1 (TSC1) and 2 (TSC2)

The tuberous sclerosis complex (TSC) is a multisystem tumor suppressor [3, 4] and its genetic autosomal dominant aberration causes non-malignant tumors to form in multiple organs, such as brain, kidney, heart, skin and lungs. TSC abnormalities usually cause neurologic disorders such as mental problems (retardation), epilepsy, delays in cognitive development, and autism. In addition to neurological disorders, other manifestation of tuberous sclerosis include facial angiofibromas, pulmonary lymphangiomyomatosis, and renal angiomyolipomas [3].

The severity and incidence of TSC can vary between patients and is inherited from a spontaneous genetic mutation or from one parent suffering from the disease. Affected parents will have half of their children most likely inheriting TSC. Either the TSC1 or TSC2 genes need to be affected for the manifestation of the disease [3, 4].

The heterodimeric complex that TSC1 and TSC2 proteins form is considered an essential integrator of numerous pathways that are involved in controlling mTOR, and particularly mTORC1 activity [4, 5]. The TSC1 gene is located on chromosome 9 and its open reading frame (ORF) encodes the 130 kDa protein TSC1 (hamartin). This protein has 1164 amino acids. On the other hand, the TSC2 gene encodes the 200 kDa protein TSC2 (tuberin), consisting of 1807 amino acids, and the gene is positioned on chromosome 16 [5]. Both activating and inhibitory phosphorylation events at particular amino acid residues are the main regulators of the TSC1 and TSC2 proteins activity [3] (Fig. 2).

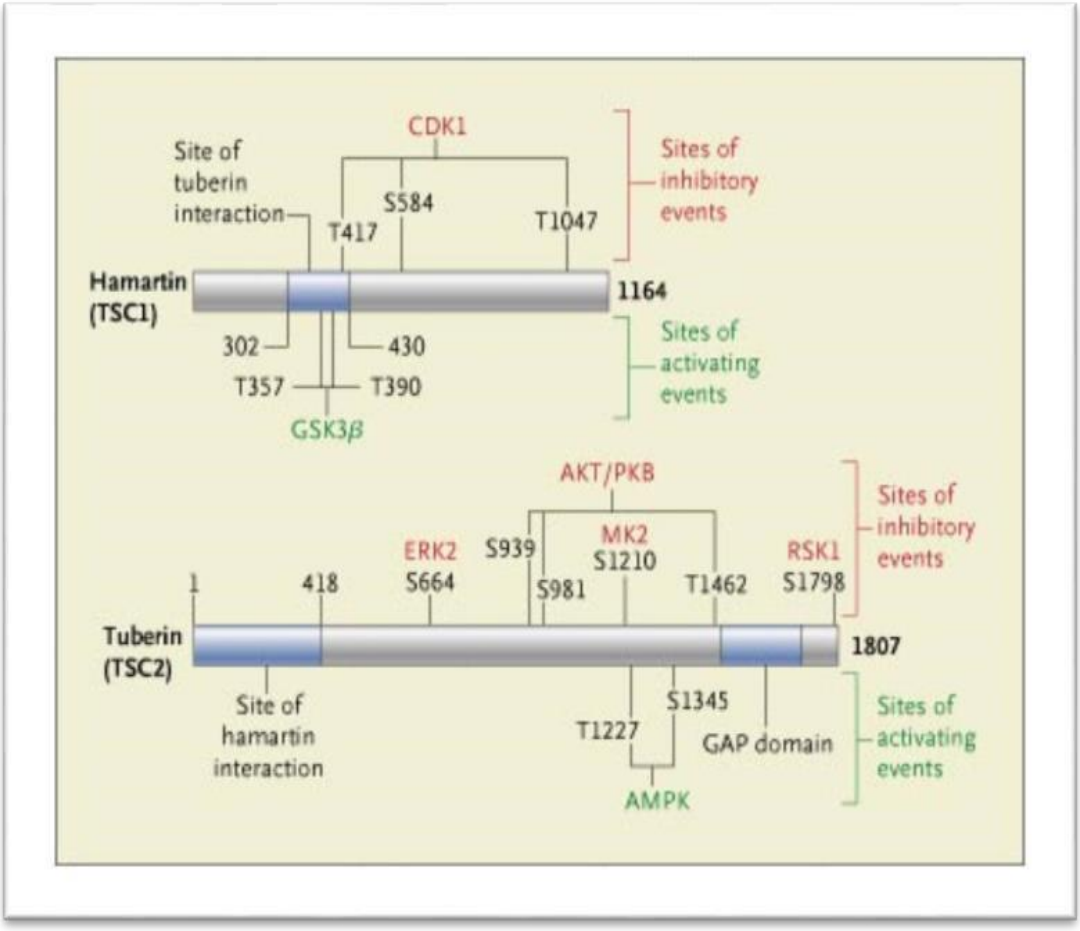

Figure 2 - Structure of TSC1 and TSC2. TSC1 (hamartin) interacts with the N-terminal 418 amino acids (aa) of the 1807 aa long tuberin through a 138 aa specific region within the N-terminal half of its 1164 amino acids. [3].

TSC2 contains a C-terminal GTPase activating protein (GAP) domain. This domain stimulates GTPase activity toward GDP-Rheb, which means that when the GTPase is activated by TSC2, it converts GTP-Rheb to GDP-Rheb. This conversion inhibits mTORC1; whereas when Rheb is in its GTP bound form it is an activator of mTORC1 [9, 10] (Fig. 3). The complex TSC1-TSC2 is inhibited by Protein kinase B (PKB/AKT) which

is a serine/threonine protein kinase that plays an important role in such as apoptosis, cell proliferation, cell migration, and transcription. This inhibition occurs through phosphorylation of TSC2 by AKT on 2-5 sites, although the mechanism at the molecular level is still unknown because the activity of GAP is not significantly affected by the various phosphorylation events [7, 8]. TSC1 prevents TSC2 from degradation, so it acts as a stabilizer of TSC2 (tuberin) [9, 10]. The adenosine monophosphate-dependent protein kinase (AMPK) usually activates the complex by phosphorylating only 2 residues of TSC2 [11] (Fig. 3).

1.2. Mammalian Target of Rapamycin (mTOR)

There are several names for mammalian (mechanistic) target of rapamycin (mTOR) such as FK506-binding protein 12-rapamycin-associated protein 1 (FRAP1). mTOR is a serine/threonine protein kinase that forms two complexes, each with specific functions. These complexes are mTORC1 and mTORC2 and are encoded by the mTOR gene [3, 5]. mTOR regulates the most important cellular functions that have direct role in cell survival such as cell growth, motility, proliferation, transcription, and protein synthesis [12]. Activation and function of mTORC1 and mTORC2 are affected in different ways by the localization of each protein because both localize to different subcellular compartments [13].

M-TORC1 is considered to be a sensor for energy, nutrition, and reduction/oxidation. It regulates protein synthesis, and is composed of different proteins, mTOR, RAPTOR, mLST8, G protein beta subunit-like (GβL), and most importantly, it is

highly sensitive to rapamycin [5] (Fig. 3). Growth factors, insulin, serum, and amino acids, stimulate the activity of mTORC1. In contrast, mTORC2 consists of mTOR, Rictor, mLST8, GβL and mSIN1 and it is considered as an essential controller of the cytoskeleton [14] (Fig. 3).

M-TORC2 also phosphorylates Akt at the serine residue S473, therefore influencing survival and metabolism [15]. Akt phosphorylation leads to a second phosphorylation, specifically at a threonine residue T308 by phosphoinositide-dependent protein kinase 1 (PDK1). These two phosphorylation events cause full activation of Akt [16, 17] (Fig. 3). The major difference between mTORC1 and mTORC2 is that mTORC1 is acutely and precisely inhibited by rapamycin, whereas rapamycin's effects on mTORC2 are more variable. Thus to produce an inhibitory effect, the drug requires chronic administration [5].

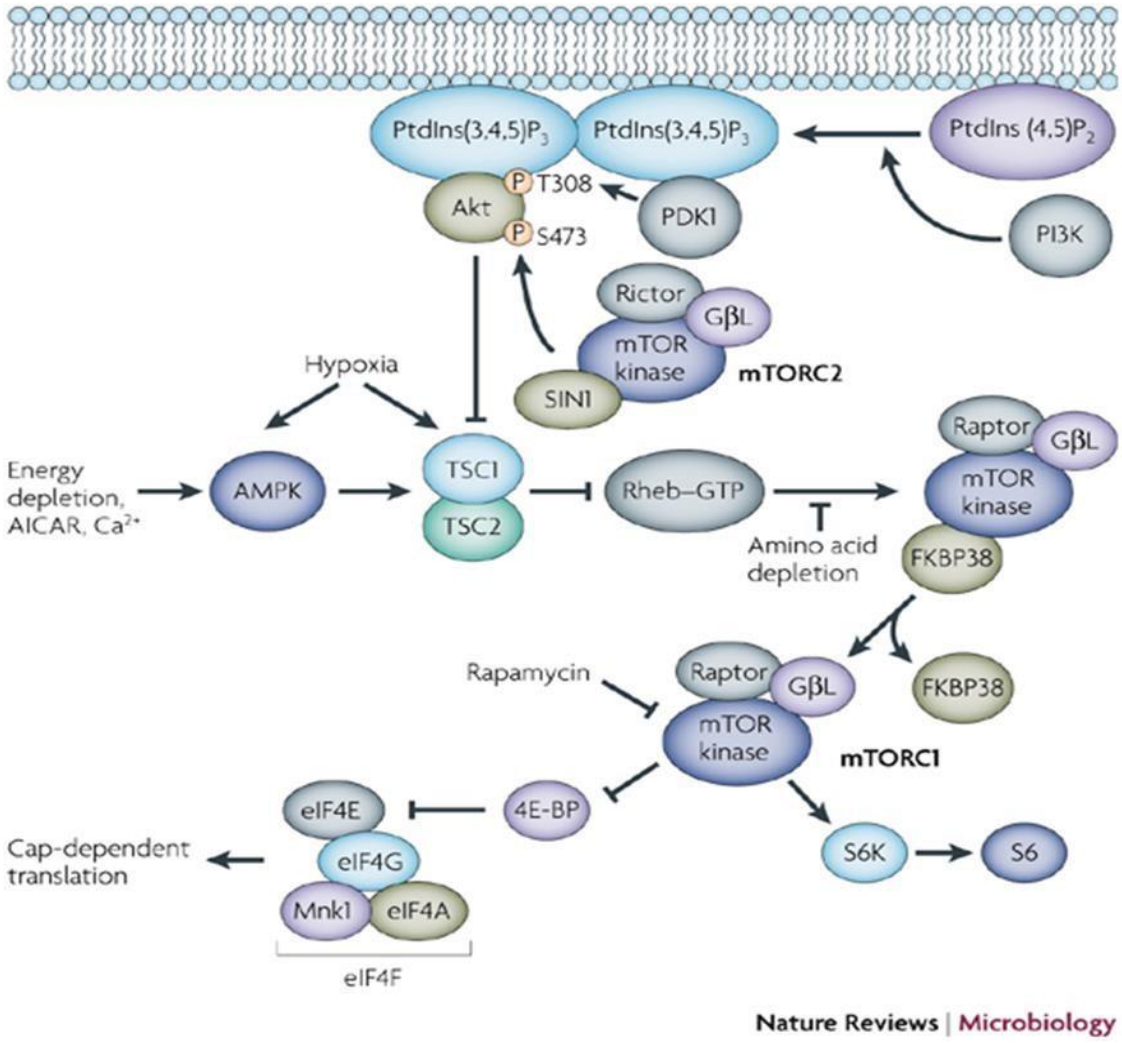

Figure 3 - PI3K–Akt–mTOR signaling [6]. The phosphatidylinositol 3'-kinase–Akt–mammalian target of rapamycin (PI3K–Akt–mTOR) pathway is shown in Figure 3. Energy or amino acid depletion, hypoxia, calcium homeostasis, rapamycin, and 5amino-4-imidazolecarboxamide ribose (AICAR) are the most important points in this pathway [6]. Abbreviations in this figure are phosphatidylinositol 3'-kinase–Akt– mammalian target of rapamycin (PI3K–Akt–mTOR); 5 amino-4-imidazolecarboxamide ribose (AICAR); eukaryotic initiation factor (eIF); Eukaryotic initiation factor 4E (eIF4E);

eIF4E binding protein (4E-BP); 4F cap-binding complex (eIF4); AMP-activated kinase (AMPK); mitogen-activated protein kinase-interacting kinase 1 (Mnk1); phosphoinositide-dependent protein kinase 1 (PDK1); phosphatidylinositol-4,5-bisphosphate (PtdIns(4,5)P2); phosphatidylinositol-3,4,5-triphosphate (PtdIns(3,4,5)P3); regulatory associated protein of TOR (raptor); rapamycin-insensitive companion of mTOR (rictor); ribosomal protein S6 (S6); p70S6 kinase (S6K); tuberous sclerosis complex (TSC).

The mechanism of mTOR inhibition by rapamycin is by association to intracellular FK506 binding protein (FKBP12) to form the FKBP12-rapamycin complex. This complex binds to an mTOR domain and this binding process causes inhibition of the mTOR activity. The most important information is that rapamycin inhibits mTORC1 in acute doses thus providing the ultimate favorable effects of the drug. However, rapamycin has a complex effect on mTORC2 because it inhibits it only in certain cell types and under extended exposure. Furthermore, the mTOR complex incorporates growth factors (IGF-1 and IGF-2), insulin, and amino acids which are considered up-stream's input pathways [18].

The mTORC1 signaling, which is commonly present in normal cells, inhibits insulin signaling by a negative feedback effect to monitor and limit the signaling of Akt. The mTORC1-S6K1 signaling leads to attenuation of PI3K activation downstream of insulin and the insulin receptor substrate proteins, IRS1 and IRS2. However, in cells responding to chronic activation of mTORC1, such as those lacking a functional TSC1-

TSC2 complex, this mechanism of negative feedback inhibits the signaling of Akt affecting its downstream pathways involved in cell survival and proliferation [4, 5].

1.3. Na^+-K^+ pump (NKP), Na^+-K^+-$2Cl^-$ cotransport (NKCC), and K^+-Cl^- cotransport (KCC)

A) Na^+/K^+ Pump (NKP)

The Na^+/K^+ Pump (sodium-potassium pump) promotes active transport of Na^+ and K^+ ions with expenditure of adenosine tri-phosphate (ATP) as cellular energy. NKP is localized in the cell membrane of most cell types and pumps three sodium ions outside of the cell and two potassium ions inside. This pump is responsible for creating ionic gradients whereby cells maintain a steady-state characterized by high concentrations of intracellular K^+ and low concentrations of Na^+, and it is not considered an anti-porter because both K^+ and Na^+ are moving against their concentration gradients. NKP, discovered in the 1950s by a Danish scientist, Jens Christian Skou, helps control the resting membrane potential, regulate cellular volume, and most importantly, functions as an integrator to regulate the mitogen-activated protein kinases (MAPK), intracellular calcium, and reactive oxygen species (ROS) [1, 19].

In the operational cycle of NKP, three Na^+ ions bind to the pump and one ATP molecule induces a conformational change which in turn moves the ions through the pump. One phosphate group from ATP remains bound to the channel, the Na^+ ions are released on the other side of the membrane and the new conformation of NKP acquires high affinity

for K^+ which binds to NKP for translocation to the intracellular compartment [1, 19]. This binding is also causing a conformational change in NKP making it to release the phosphate group into the cytoplasm. This process allows NKP to change to its original conformation and as a result, the K^+ ions will be released into the cell. In its normal conformation, NKP has a high affinity for Na^+ ions but it is only when these ions bind to the pump that another cycle is initiated. The movement of Na^+ and K^+ against their concentration gradients, i.e. from low to high concentrations is only possible by constant consumption of ATP by the pump [1, 2, 19].

NKP is a heterotrimer containing three subunits: α, β, and γ [20]. The alpha subunit has a molecular mass of 112 kDa, is considered a multispanning membrane protein, and is responsible for the transport properties of the enzyme. The α-subunit contains the binding sites for ATP, cations, and ouabain [21].

There are four α-subunits which are α1, α2, α3, and α4 in animal cells, the α2 subunit is the more abundantly expressed and is the most sensitive to ouabain. However, in humans, α1 is the most sensitive to this drug. The β-subunit is a polypeptide of 40-60 kDa molecular weight, and crosses the plasma membrane. This subunit is crucial for the activity of the Na^+/K^+ ATPase [20-22]. A third protein, the γ-subunit, serves as a pump regulator [20, 21].

B) Na^+-K^+-2Cl^- Co-transport (NKCC)

The membrane-bound NKCC protein plays a critical role in variety of epithelial process, namely absorption and secretion. Beside that NKCC promotes bidirectional transport of Na^+, K^+, and 2 Cl^- ions. NKCCs are strongly involved in cell volume and cell cycle regulation. Two NKCC isoforms are currently known. While NKCC2 seems to be present restrictively in the kidney, NKCC1, the house-keeping form, is present in almost all cells [20, 22, 28, 29].

There are two different genes (SLC12A2 and SLC12A1) encoding NKCC1 and NKCC2, respectively, see Table 1. NKCC transports Na^+, K^+ and Cl^-, and can be blocked by bumetanide, a loop diuretic. NKCC is not driven by a membrane voltage because it is electroneutral requiring Na^+, K^+, and 2Cl^- to be present simultaneously on the same side of the cell membrane to be transported in or out of the cells, depending on the ionic gradients [20, 22, 29]. One ion increases the affinity for the other ions to bind to NKCC when a Na^+, K^+, or Cl^- ion is binding to the cotransport. More specifically Na^+ binds first and then Cl^-, followed by K^+ and a second Cl^- externally. According to the "gliding symmetry model", internally, the Na^+ is released first and then the first Cl^-, followed by the K^+ and finally by the second Cl^- [48]. In other words, ions depend on each other to increase the binding site affinity for the remaining ions. NKCC is activated by phosphorylation and deactivated by de-phosphorylation. Phosphorylation of NKCC is mediated by protein kinase C (PKC), protein kinase A (PKA), with no lysine kinase (WNK), and Ste20-related proline-alanine-rich kinase (SPAK) [34], whereas de-phosphorylation is mediated by protein phosphatases.

Moreover, the concentrations of ions such as Cl^-, Na^+, Ca^{2+}, K^+, and Mg^{2+} directly affect NKCC activity [20, 22, 28-30].

Gene	Species	Gene Symbol
NKCC1	Mouse	Slc12a2
NKCC2	Mouse	Slc12a1

Table 1 - Genes encoding the Na^+-K^+-$2Cl^-$ cotransporters.

C) K^+-Cl^- Co-transport (KCC)

KCCs promote electroneutral K^+ and Cl^- cotransport and are involved in the Na^+-independent K^+ transport into or out of the cell, depending on the ionic gradient. KCCs preserve intracellular Cl^- and K^+ homeostasis, and ultimately maintain cell volume [20, 22, 30, 31].

The Cl^--dependent K^+ transport system was first recognized in sheep and fish red blood cells (RBCs) as a swelling-activated K^+ flux [26, 27, 49, 63, 64, 65]. KCCs have four protein isoforms KCC1 to KCC4 and are encoded by four genes SLC12A4 to 7 respectively, possessing splice variants in each isoform. The KCC1 gene is located on chromosome 16.q22.1, and its ORF translates a 1085 amino acids protein that fulfills house-keeping function by regulating volume homeostasis in most tissues [36, 37, 65]. KCC2, located on chromosome 20, occurs in two spliced variants KCC2a and KCC2b. KCC2b, which is only present in the brain, whereas the second and longer variant KCC2a occurs not only in the brain but also in other tissues such as the lens and myocardium [20, 22, 26,

27, 36, 37, 65] . The third isoform is KCC3 and it is located on chromosome 15.q13. It is usually found in skeletal muscle, brain, heart, pancreas and kidney. KCC3 has two major isoforms, KCC3a which has 1150 amino acids, and KCC3b that has 1099 amino acids, both mainly expressed in the kidney [20, 22, 36, 37].

The last isoform, KCC4 which has 1083 amino acids, located on chromosome 5p15, and is expressed in different tissues such as thymus, spleen, spinal cord, brain, bone marrow, pancreas, liver, skeletal muscle, lung, and the heart. KCCs function can be appreciated when the extracellular medium becomes hyposmotic, inducing water to enter the cell and causing an increase in cell volume. This activates volume-sensitive K^+ and Cl^- channels and the KCCs, which extrude K^+ and Cl^- ions and water in order to bring the volume of the cell back to its original volume [20, 22, 23, 65]. Along with regulating cell volume, KCCs have been found to be involved in numerous pathologies, cell migration, and cell growth [38]. KCCs also play important roles in sickle cell disease, cardiovascular diseases, and tumor biology [33, 61, 62, 63, 64, 65].

2. Hypothesis and Specific Aims

2.1. Background for hypothesis

The two functionally important genes TSC1 and TSC2 in MEFs are positioned on chromosomes 9q34 and 16p13.3, respectively, and encode the 130 kDa hamartin and 200 kDa tuberin proteins, respectively [3, 4]. MEFs TSC1-KO and TSC2-KO cells have high mTORC1 activity [4, 5] that may lead to activation of NKCC [41, 42] and deactivation of

KCC [43, 44] as we expected. Therefore, NKCC's and KCC's activities should be increased and decreased with respect to WT cells. Our studies showed activation of NKCC through increased Rb^+ (K^+) influx and deactivation of KCC through decreased Rb^+ (K^+) influx. Based on these data, we propose the following hypothesis.

2.2. Hypothesis

The TSC1 and TSC2 genes, which control cell processes through the mTOR pathway, are important for K^+ homeostasis and transport through the Na^+/K^+ Pump (NKP), Na^+-K^+-Cl^- (NKCC) and K^+-Cl^- (KCC) cotransports in mouse embryonic fibroblasts (MEFs).

I) Specific Aim 1

Determine the optimal conditions for K^+ movements requiring metabolic energy (Na^+/K^+ pump) to assess the role of the TSC1 and TSC2 genes and the mTOR pathway on K^+ homeostasis. This will be accomplished by determination of the optimal ouabain concentration for Rb^+ influx and K_i content in WT, TSC1-KO, and TSC2-KO MEF cells.

II) Specific Aim 2

Determine the optimal conditions for K^+ movements through pathways indirectly dependent on metabolic energy (Na^+-K^+-Cl^- and K^+-Cl^- cotransport) to assess the role of the TSC1 and TSC2 genes and the mTOR pathway on K^+ homeostasis. This will be

accomplished by determination of the optimal bumetanide concentration for Rb^+ influx and K_i content in WT, TSC1-KO, and TSC2-KO MEF cells.

III) Specific Aim 3

Determine K^+ movements under physiological conditions to assess the role of the TSC1 and TSC2 genes and the mTOR pathway on K^+ homeostasis and to determine whether they behave as expected for adult Mouse cells. This will be accomplished by characterization of Rb^+ (K^+) influx and K_i content in the presence and absence of inhibitors of NKP, NKCC, and KCC at their optimal concentrations in WT, TSC1-KO and TSC2KO MEF cells.

3. Materials and Methods

3.1. Cell Models

These cell models were provided by Dr. Kristopher T. Kahle, M.D. Ph.D. from Harvard Medical School. Wild type (WT) MEF cells were used as controls. These cells possess non tumorigenic characteristics [39], normal cell size and become confluent in about 4 days, according to our observations. TSC1-KO and TSC2-KO MEF cells are used as a model of increased mTORC1 activity and S6K expression, accelerated cell proliferation and growth, and are tumorigenic [3]. According to our observations, these cells become confluent in about 2 days and are of larger size than WT cells.

3.2. Chemicals

Chemicals used in this study were: From Fisher Scientific: sodium chloride (NaCl), potassium chloride (KCl), magnesium chloride ($MgCl_2$), sucrose, sodium hydroxide (NaOH), D-glucose, 70% perchloric acid (70% PCA), bicinchonic acid (BCA) protein assay reagents, and Tri-hydroxyamino methane (Tris) free base. Magnesium gluconate was from Sigma-Aldrich (St. Louis, MO). Chemicals from J.T.Baker Chemical Co (Center valley, PA) were: calcium chloride ($CaCl_2$), anhydrous and (4-(2-hydroxyethyl)-1piperazine ethane sulfonic acid (HEPES) free acid. High purity rubidium chloride (RbCl) 99.9% and amidosulfonic acid (sulfamic acid, S) were purchased from Alfa Aesar (Ward Hill, MA); Cesium chloride (CsCl) from Life technologies (Carlsbad, CA) and calcium gluconate from Acros Organics (NJ).

3.3. Inhibitors

Ouabain octahydrate was from Calbiochem (San Diego, CA) and bumetanide was from Sigma-Aldrich (St. Louis, MO).

3.4. Solutions for flux studies

Washing solutions

Balanced salt solution with sodium chloride (BSS-NaCl) (mM): 20 Hepes-Tris, 5 KCl, 2 $CaCl_2$, 1 $MgCl_2$, 10 glucose and NaCl, pH 7.4, 37 °C, 300 mOsM.

Balanced salt solution with sodium gluconate (BSS-Na^+ gluconate) (mM): 20 Hepes-Tris, 5 K^+ gluconate, 2 Ca-gluconate, 1 Mg-gluconate, 10 glucose and Na^+-gluconate, pH 7.4, 37 °C, 300 mOsM.

Pre-incubation solutions

Balanced salt solution with sodium chloride and bovine serum albumin (BSS-NaCl-BSA) (mM): 20 Hepes-Tris, 5 KCl, 2 $CaCl_2$, 1 $MgCl_2$, 10 glucose, 0.1 % BSA and NaCl, pH 7.4, 37 °C, 300 mOsM.

Balanced salt solution with sodium gluconate and bovine serum albumin (BSS-Na^+ gluconate-BSA) (mM): 20 Hepes-Tris, 5 K^+ gluconate, 2 Ca gluconate, 1 Mg gluconate, 10 glucose, 0.1 % BSA and Na^+ gluconate, pH 7.4, 37 °C, 300 mOsM.

Flux solutions

Balanced salt solution with rubidium chloride, sodium chloride, and bovine serum albumin (BSS-RbCl-NaCl-BSA) (mM): 20 Hepes-Tris, 10 RbCl, 2 $CaCl_2$, 1 $MgCl_2$, 10 glucose, 0.1 % BSA and NaCl, pH 7.4, 37 °C, 300 mOsM.

Balanced salt solution with rubidium sulfamate, sodium gluconate, and bovine serum albumin (BSS-RbS-Na^+ gluconate-BSA) (mM): 20 Hepes-Tris, 10 Rb^+ sulfamate, 2 Ca gluconate, 1 Mg gluconate, 10 glucose, 0.1 % BSA and Na^+ gluconate, pH 7.4, 37 °C, 300 mOsM.

Final wash solution

10 mM of 3-(N-Morpholino) propane sulfonic acid (MOPS)-Tris, $MgCl_2$, pH 7.4, 37 °C, 300 mOsM.

Rb^+ Extraction

5 % perchloric acid, 4 mM CsCl

Protein dissolution

1M NaOH

3.5. Cell cultures

Mouse embryonic fibroblasts (MEFs) WT, TSC1-KO, and TSC2-KO were cultured in Dulbecco's Modified Eagle (DMEM) high glucose medium + L-glutamine + 110 mg/L sodium pyruvate (Life Technologies, Catalog No.11995-073) supplemented with 10 % premium fetal bovine serum (FBS) (Atlanta Biologicals, Catalog No.S11150), 100 units/ml penicillin (Hyclone, Catalog No. SV30010), 100 µg/mL streptomycin (Hyclone, Catalog No. SV30010) in a humidified incubator with 5 % CO_2 at 37 °C. Washing buffer 1X phosphate buffer solution (PBS) (8 g NaCl + 0.2 g KCl + 1.44 g Na_2HPO4 + 0.24 g KH_2PO4 dissolved in 1000 ml deionized H_2O, pH 7.4) and 0.5 % TrypsinEDTA as to remove adherent cells from a culture surface (Life Technologies, Catalog No.15400-054). Cell freezing was done in dimethyl sulfoxide (DMSO, Life Technologies, Catalog No.D8418-50) at a concentration of 10 % of the freezing medium.

3.6. BCA Protein Assay

Proteins were determined by the bicinchoninic acid (BCA) assay, BCA™, consisting of two reagents, Protein Assay Reagent A (50 parts) and B (1 part), and is a colorimetric assay that detects proteins by changing color from green to purple [24]. Proteins in the NaOH extract were determined by adding 12.5 µl aliquot to each well of a 96-well microplate (Life Technologies, catalog # 23252) by using an electronic pipette. The 96-well plate was incubated for 30 min at 37 °C and cooled down for 10 min at RT following quantification by using a Labsystems MultiskanMCC/340 plate reader, according to the manufacturer's instructions.

3.7. Ion Flux Studies

Ion fluxes were determined according to previously published protocols [25, 26, 27] with some modifications. Cells were grown to 85 % confluence in 12-well plates. WT, TSC1-KO, and TSC2-KO MEFs were removed from the incubator, the culture medium was aspirated, cells were washed three times with 1mL of 300 mOsM BSS-NaCl or BSS-Na^+ gluconate and then equilibrated in BSS-BSA-NaCl or BSS-BSA-Na^+ gluconate, pH 7.4, 37 °C for 10 min, thereafter supernatants were removed and then exposed to pre-warmed flux media BSS-BSA-RbCl or BSS-BSA-RbS for pre-determined time points (2.5 min to 10 min). Thereafter, cells were washed with washing solution at room temperature (RT) to block Rb^+ influx or K_i loss. Cellular Rb^+ and K^+ were extracted after cell lysis by exposing them for 15 min to ice cold 5 % PCA + 4 mM CsCl, the remaining solution was aspirated and protein was extracted by dissolving the attached cells in 1 M NaOH. Rb^+ and

K^+ were measured by atomic emission and absorption spectrophotometry, respectively using a Perkin Elmer 5000 Atomic Absorption Spectrophotometer. Protein was determined by the BCA assay [24] as described above. Rb^+ uptake or K_i content were calculated in nmoles/mg protein as a function of time. Where indicated, ouabain (2 mM) and bumetanide (20 μM) were added to the flux media to block NKP and NKCC, respectively. The ouabain- and the bumetanide-sensitive Rb^+ influx in Cl^- medium are defined as NKP and NKCC, respectively, whereas KCC is defined as the (ouabain + bumetanide)-insensitive Cl^--dependent Rb^+ influx and was obtained by subtracting the Rb^+ influx in Cl^- medium minus that in non-Cl^- medium (sulfamate or gluconate replacement) containing the two inhibitors

.

3.8. Statistical Analysis

STATISTIX 7 software, (Graphpad Software, La Jolla CA) and (Analytical software, Tallahassee FL) from Graphpad Prism 5. These programs were used to determine statistical significance by one-way ANOVA, Wilcoxon signed rank test, Kruskal-Wallis ANOVA, and paired or unpaired t-test. Graphs, diagrams, and charts were plotted using Origin 7 software and Origin Pro 8.5 Student Version (Origin Labs, Northampton MA). Data were considered statistically significant for p-values < 0.05.

4. Results

The purpose of this study was to understand the role of the TSC1 and TSC2 genes and their control of the mTOR signaling pathway on K^+ homeostasis. To this end, we used

cellular models lacking each of the genes and their respective controls, i.e. WT, TSC1-KO and TSC2-KO MEF cells, and determined the function of key transporters known to be involved in the maintenance of K^+ and cellular volume homeostasis, and in cell migration and proliferation. The transporters are the Na^+/K^+ pump and the Cl^--coupled Na^+ and K^+ co-transporters, i.e. NKP, NKCC and KCC. In addition, the TSC1 and TSC2 genes and their products hamartin and tuberin, respectively, control cell processes through the mTOR pathway which is important for cell migration, proliferation, and protein synthesis. Therefore, we proposed that the TSC1 and TSC2 genes and the mTOR pathway play a significant role in regulating NKP, NKCC and KCC. Thus, as we hypothesized, the TSC1 and TSC2 genes are expected to play a significant role in regulating cell K^+ and Cl^- homeostasis and cellular volume. We assessed K^+ homeostasis through the activities of NKP, NKCC and KCC determined by rubidium (Rb^+, a K^+ congener) influx and K_i content in the presence and absence of the NKP inhibitor ouabain, the NKCC inhibitor bumetanide and by the Cl^--dependent Rb^+ influx via KCC.

The results are presented with a logic dictated by the scant information available for these cell models regarding the conditions under which to determine Rb^+ influx and K_i content; this information was mostly borrowed from knowledge of other cultured cells. Because of the novelty of our studies, we determined the parameters in question in the absence and presence of inhibitors under different conditions to learn whether MEF cells behave like adult murine cells (Specific Aims 1-3). It was also necessary to determine the optimal concentrations of the inhibitors ouabain and bumetanide to measure Rb^+ influx and K_i content in MEF cells (Specific Aims 1 and 2). Lastly, the characterization of Rb^+ (K^+)

influx and K_i content was done under physiological conditions applying the knowledge gained in the preceding studies to determine whether the TSC1 and TSC2 genes are determinants of K^+ homeostasis through the mTOR pathway in MEF cells (Specific Aim 3).

4.1. Rb^+ influx and K_i content in WT, TSC1-KO and TSC2-KO in MEF cells in the absence of inhibitors.

Previous studies in MEF cells provide information on ion transport and cell migration. For instance, iron homeostasis is regulated by mTOR through modulation of the transferrin receptor 1 (TfR1) stability and by altering cellular iron transport [50]. Inversin controls cell migration processes through transcriptional regulation of genes that control cytoskeletal organization and ion transport [51]. Presenilin expression affects copper and zinc transport in MEF cells [52]. However, no detail studies on K^+ homeostasis in MEF WT, TSC1-KO, and TSC2-KO have been done. The present study was designed to fill this gap in knowledge. Thus, an initial step was to assess the relative magnitudes of Rb^+ influx and intracellular K^+ in WT, TSC1-KO, and TSC2-KO MEF cells in the absence of inhibitors to determine the baseline values of these parameters for the three cell types [Figure 4].

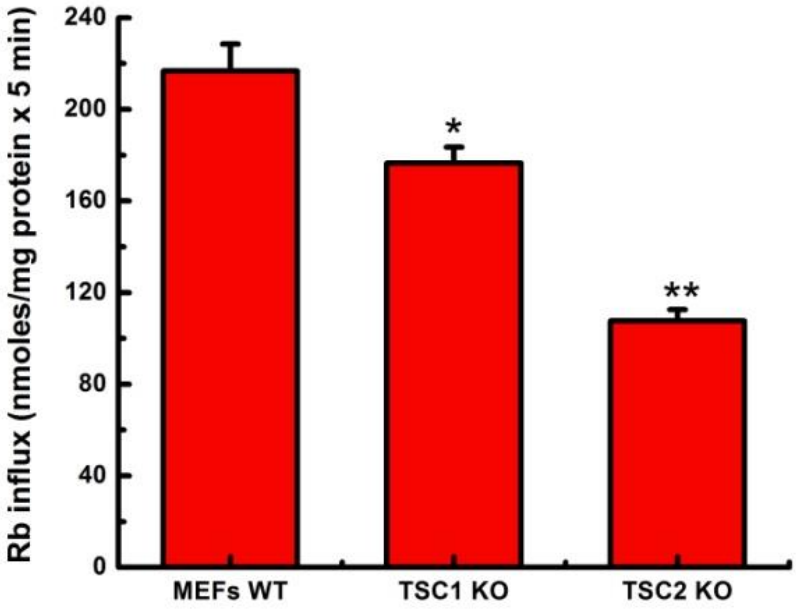
Rb influx (nmoles/mg protein x 5 min)
240
200
160
120
80
40
0
*
**
MEFs WT
TSC1 KO
TSC2 KO

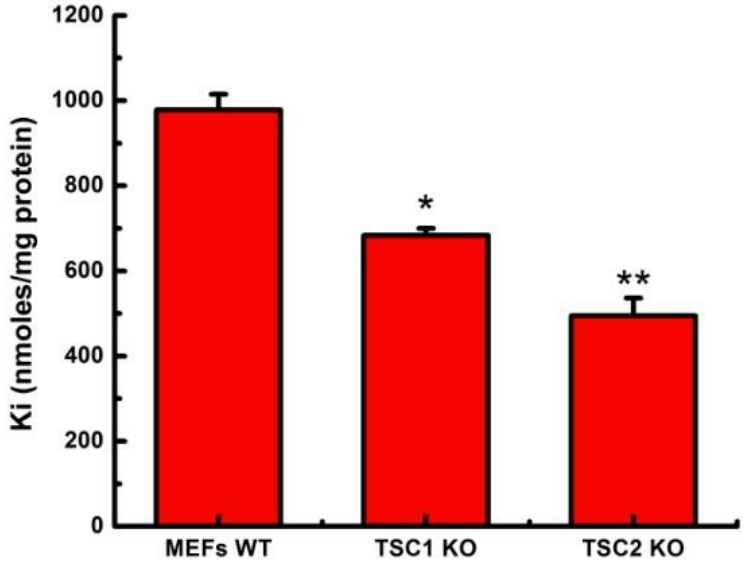
Ki (nmoles/mg protein)
1200
1000
800
600
400
200
0
*
**
MEFs WT
TSC1 KO
TSC2 KO

Figure 4 – Rb^+ influx and K_i content in WT, TSC1-KO and TSC2-KO in MEF cells in the absence of inhibitors. Rb^+ influx was determined as described in Materials and Methods. Flux time, 5 min. Number of individual determinations (n) for WT, TSC1-KO , and TSC2-KO cells were n = 14, 21 and 16, respectively. Values are means ± S.E. Details are discussed in the text.

Both the Rb^+ influx and K_i content for the three cell types were statistically different and followed the sequence WT > TSC1-KO > TSC2-KO MEF cells suggesting that cells lacking or with abnormalities in the TSC2 gene cause more detrimental effects on K^+ homeostasis than the TSC1 gene. This finding is in line with the fact that abnormalities in the TSC2 gene are more severe and common in the TSC patient population [3, 53, 54, 55, 56].

4.2. Studies on the Na^+/K^+ pump activity in WT, TSC1-KO and TSC2-KO in MEF cells.

Due to lack of information in the literature concerning the optimal conditions to measure the activity of NKP in WT, TSC1-KO, and TSC2-KO MEFs, the first step was to do ouabain dose-response (ODR) curves for Rb^+ influx [Figures 5 and 6] and K_i content [Figures 7 and 8] to determine the maximal ouabain inhibitory concentration (OS_{max}). Figure 5 shows inhibition of Rb^+ influx at the ouabain concentrations tested (0-2.5 mM) for the 3 cell types with the relative values of Rb^+ influx following the sequence WT > TSC1-KO > TSC2-KO at 0 mM ouabain whereas that of the mean values obtained by averaging the Rb^+ influx from the ODR curves for each cell type was WT ~ TSC1-KO > TSC2-KO.

The effect of ouabain on K_i content and its averages from ODR curves done in WT, TSC1-KO and TSC2-KO MEF cells are represented in Figures 7 and 8, respectively. As expected for cellular K^+, increasing the ouabain concentration did not affect K_i content in WT and TSC1-KO cells (Figure 7) because K^+ enters the cell through NKP but exits through other pathways (K^+ channels, NKCC, KCC and others), which are not sensitive to ouabain. In contrast, in TSC2-KO cells, K_i content decreased with increasing ouabain concentrations, which is unexpected in light of the findings in WT and TSC1-KO cells. In addition, TSC2-KO cells lost about 80 % of the intracellular K^+ with respect to WT cells (Figure 8). These results albeit unexpected once more confirm that lack of or abnormalities in the TSC2 gene appear to have detrimental effects on K^+ homeostasis.

a) Determination of the optimal ouabain concentration for Rb^+ influx and K_i content in WT, TSC1-KO, and TSC2-KO.

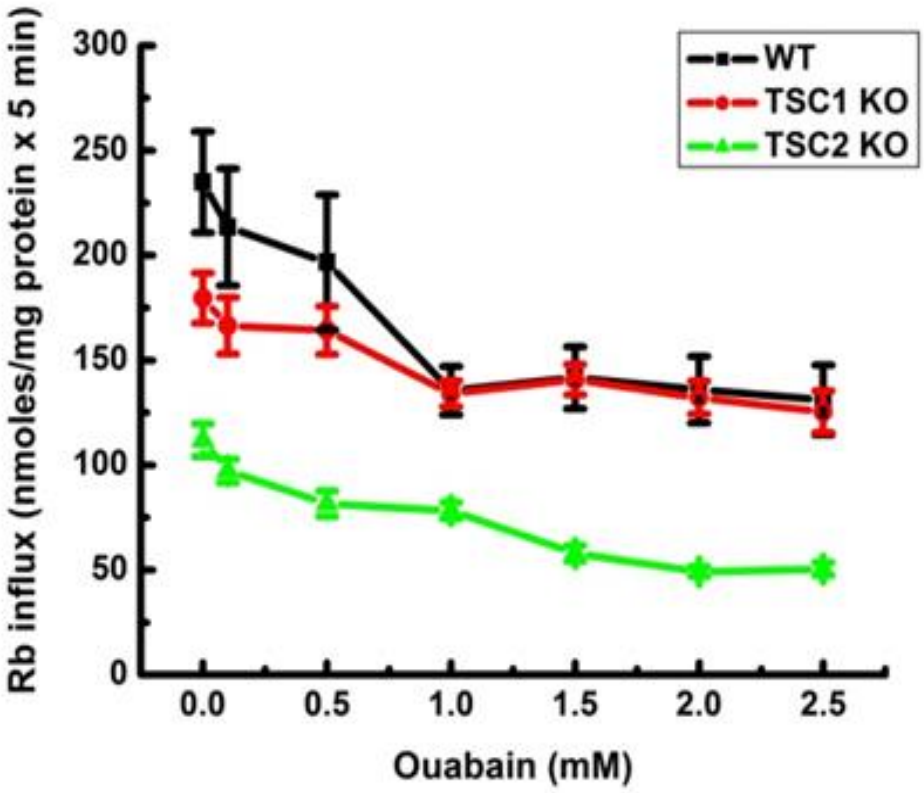

Figure 5 - Ouabain-dose response (ODR) of Rb^+ influx in WT, TSC1-KO, and TSC2-KO MEF cells. Rb^+ influx was determined as described in Materials and Methods. Flux time, 5 min. Number of individual determinations (n) for WT, TSC1-KO , and TSC2-KO cells were n = 6, 12 and 6, respectively. Values are means ± S.E. Details are discussed in the text.

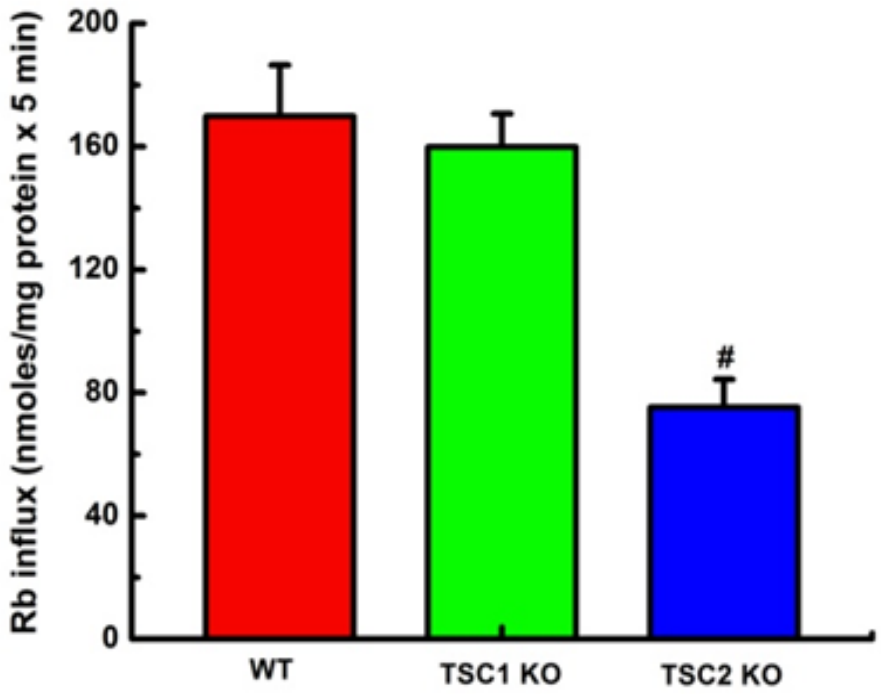

Figure 6 – Rb^+ influx averages from ouabain dose-response of Rb^+ influx in WT, TSC1-KO, and TSC2-KO MEF cells. Rb^+ influx was determined as described in Materials and Methods. Flux time, 5 min, Rb^+ influx averages in this figure were calculated as the sum of all the values of Rb^+ influx at each ouabain concentration (0, 0.1, 0.5, 1, 1.5, 2, 2.5 mM) divided by the number of ouabain concentrations used (7 for each cell line). Number of individual determinations (n) for WT, TSC1-KO, and TSC2-KO cells were n = 6, 12 and 6, respectively. Values are means ± S.E. Details are discussed in the text.

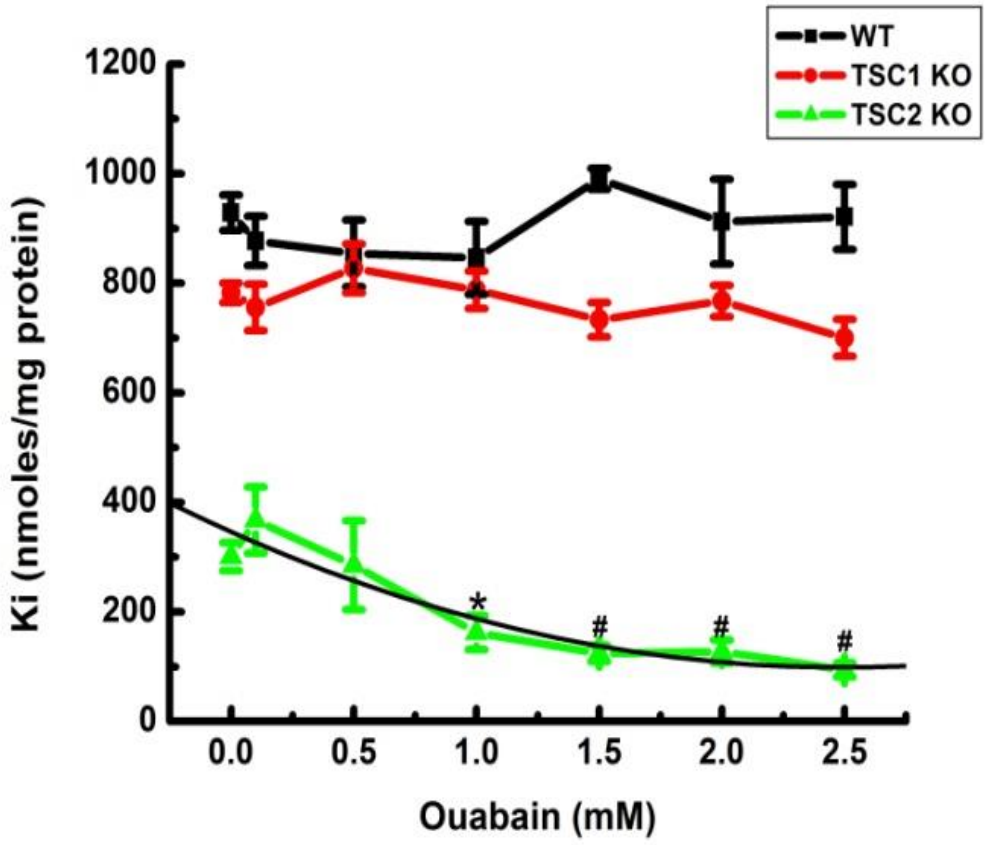

Figure 7 - Effect of increasing concentration of ouabain on K_i content in WT, TSC1-KO, and TSC2-KO MEF cells. K_i content was determined as described in Materials and Methods after 5 min exposure to the indicated ouabain concentrations. Number of individual determinations (n) for WT, TSC1-KO, and TSC2-KO cells were n = 6, 12 and 6, respectively. Values are means ± S.E. Details are discussed in the text.

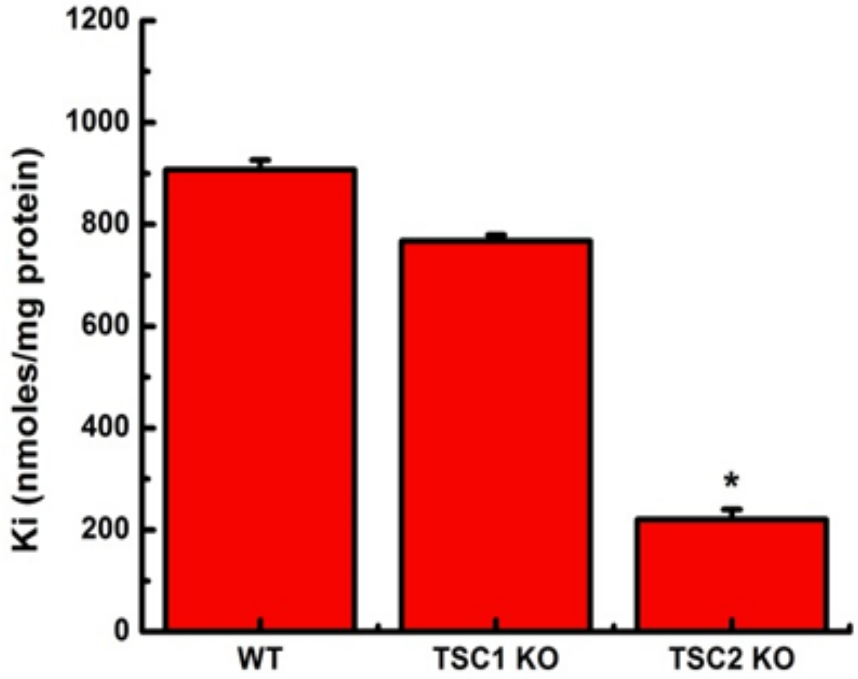

Figure 8 – Averages of K_i content from ouabain dose-response curves in WT, TSC1-KO, and TSC2-KO MEF cells. K_i content was determined as described in Materials and Methods after 5 min exposure to the indicated ouabain concentrations. Number of individual determinations (n) for WT, TSC1-KO, and TSC2-KO cells were n = 6, 12 and 6, respectively. Values are means ± S.E. Details are discussed in the text.

As shown in figures 4-8, there were statistically significant differences in the response of TSC1-KO and TSC2-KO cells to ouabain. However, it was not clear whether the differences were due to the maximal ouabain inhibition, as it appears to be from the figures, and/or to differences in the sensitivity of the mutant cells to ouabain (the half

maximal ouabain inhibitory concentration (OIC_{50}), Therefore, it was necessary to further characterize the effect of the TSC1 and TSC2 genes on K^+ homeostasis and the response of the mutants to ouabain. To this end the maximal ouabain-sensitive (OS_{max}) and OIC_{50} were determined for Rb^+ influx and K_i content in the three cell types.

Figure 9 represents the calculated ouabain-sensitive (OS) Rb^+ influx (NKP activity) from ODR curves as a function of the ouabain concentration for WT, TSC1-KO and TSC2-KO MEF cells. The figure shows that inhibition of NKP activity in WT and TSC1-KO cells reach saturation at 2 mM ouabain, when the OS_{max} of WT cells is 121 nmoles/mg protein x 5 min whereas that of TSC1-KO is about 50 % less than that. In contrast, inhibition of NKP by ouabain in TSC2-KO cells does not appear to saturate even at 2.5 mM ouabain and its value at that concentration is also 50 % of the WT. Because higher doses of ouabain caused cell detachment and were toxic to the cells, 2.5 mM was the highest dose used in this study (Figure 9 and Table 2). A plausible explanation for these findings will be given in the Discussion. The main message from these data is again that lack or abnormalities in the TSC1 and TSC2 genes lead to abnormal activity of one of the major pathways involved in K^+ homeostasis, i.e. NKP.

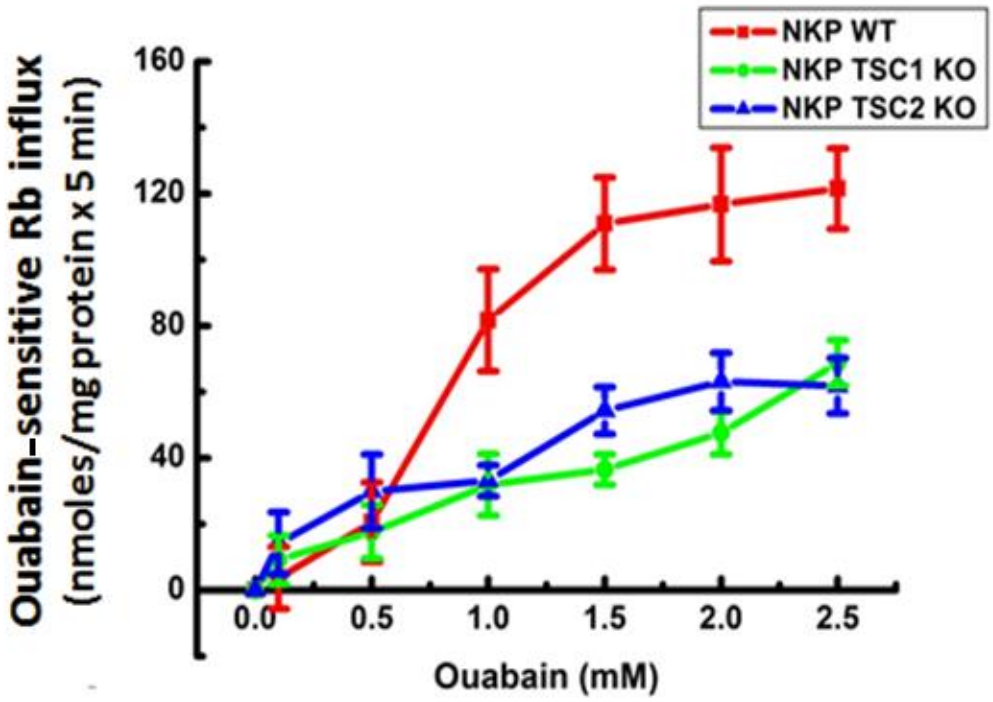

Figure 9 - Determination of the maximal ouabain inhibitory concentration (OS_{max}). Rb^+ influx was determined as described in Materials and Methods and the ouabain-sensitive (OS) flux was calculated from ODR curves (see Figure 5) for each ouabain concentration. The OS_{max} was determined as the lowest dose saturation was reached. Flux time, 5 min. Number of individual determinations (n) for WT, TSC1-KO, and TSC2-KO cells were n = 6, 12 and 6, respectively. Values are means ± S.E. Details are discussed in the text.

Studies in rat cells have shown that the α2 isoform of the Na^+/K^+ ATPase has higher affinity than α1 isoform for ouabain, in which the IC_{50} for α2 isoform is 0.01 – 0.5 mM and for α1 isoform is more than 10 mM [40]. The results shown in this study appear to be no

exception at least for the affinity for α2 isoform. To further assess the sensitivity of NKP to ouabain in the cell models in question, the half maximal ouabain inhibitory concentration (OIC_{50}) was determined by assigning a value of 100 % to the OS_{max} for each WT, TSC1-KO and TSC2-KO MEF cell type and calculating the percentages for each ouabain concentration shown in Figures 5-9.

Figure 10 and the OIC_{50} values were obtained. As we can see in figure10 and Table 2, the OIC_{50}s in WT, TSC1-KO, and TSC2-KO are approximately 0.5, 0.6, and 0.6 mM, respectively, which are not statistically significantly different given the large dispersion in the data shown in Table 2

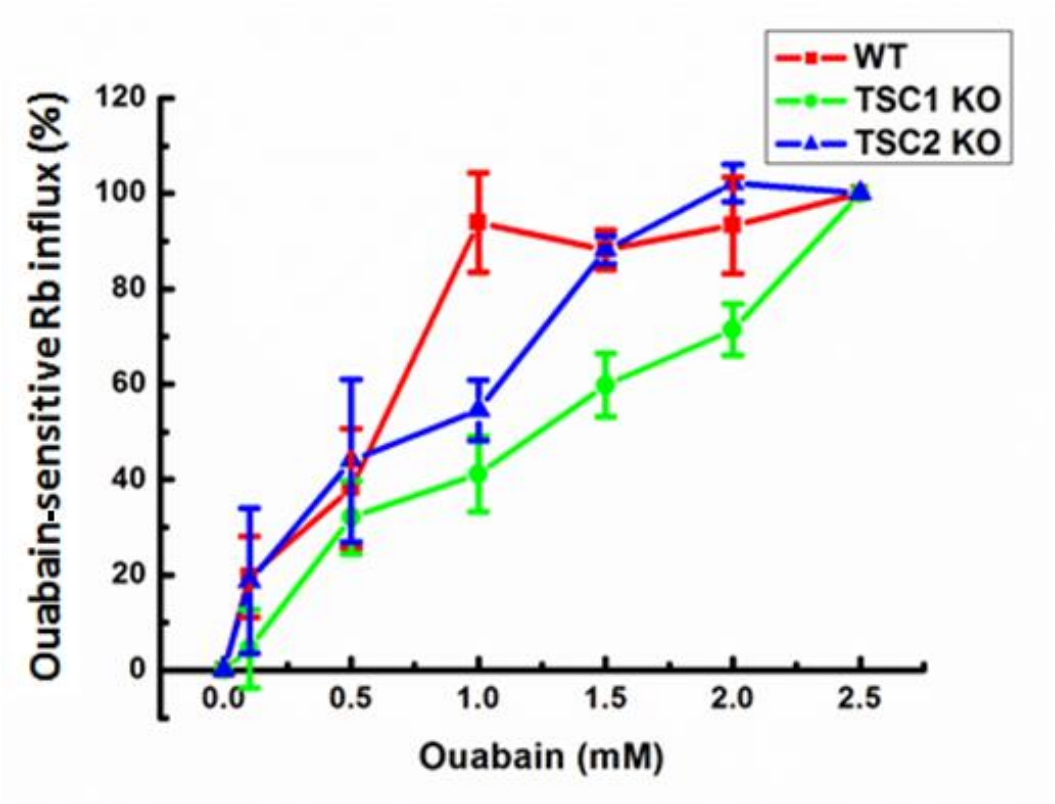

Figure 10 - Determination of the half maximal ouabain inhibitory concentration (OIC_{50}). Rb^+ influx was determined as described in Materials and Methods and the ouabain-sensitive (OS) flux was calculated from ODR curves (see Figure 5) for each ouabain concentration. Ouabain-sensitive Rb^+ influxes were calculated as percent of the OS_{max}, which was assigned arbitrarily a 100 % value. The OIC_{50} values were obtained from the fitted curved at the 50 % value. Flux time was 5 min. Number of individual determinations (n) for WT, TSC1-KO, and TSC2-KO cells were n = 6, 12 and 6, respectively. Values are means ± S.E. Details are discussed in the text.

A summary of the ouabain effects on the Rb^+ influx parameters described above is shown in Table 2 for WT, TSC1-KO and TSC2-KO MEF cells.

b) Summary of ouabain-dose-response of Rb^+ Influx, OIC_{50} and OS_{max} in WT, TSC1-KO and TSC2-KO MEF cells.

Half maximal ouabain inhibitory concentration (OIC_{50}) and maximal ouabain-sensitive Rb^+ influx (OS_{max}), which are obtained for WT, TSC1-KO, and TSC2-KO cells, have been summarized in Table 2 to determine whether there is a difference in these parameters between the three cell types, in addition to other statistical variables. The table also lists the standard error (SE), range (minimum and maximum values) standard deviation (SD), number of individual determinations (n) and independent experiments (N) performed for WT, TSC1-KO, and TSC2-KO cells.

Cells	**WT**	**TSC1-KO**	**TSC2-KO**
OIC_{50}	**0.515**	**0.637**	**0.624**
SE	**0.17**	**0.14**	**0.42**
RANGE	**0.34 to 0.69**	**0.29 to 0.99**	**0.199 to 1.05**
SD	**0.24**	**0.29**	**0.6**
OS_{max}	**121.53**	**58.54 ****	**61.84 ****
SE	**12.99**	**4.71**	**12.34**
RANGE	**108.54 to 134.53**	**48.36 to 66.83**	**49.5 to 74.18**
SD	**18.37**	**9.42**	**17.45**
n	**6**	**12**	**6**
N	**2**	**4**	**2**

Table 2: Maximal ouabain-sensitive (OS_{max}) Rb^+ influx (nmol/mg protein x 5 min) and half maximal ouabain inhibitory concentration (OIC_{50}, mM), statistical parameters and number of individual determinations (n) and independent experiments (N) performed for WT, TSC1-KO, and TSC2-KO cells.

The conclusion from these data is that the OS_{max} was decreased by 50 % in the mutants whereas the affinity for ouabain was not altered. The underlying factor/s leading to a decrease in the maximal inhibition by ouabain in the absence of the TSC1 and TSC2 genes could be explained by deregulation of the mTOR pathway, as it will be explained in the Discussion.

4.3. Studies on NKCC activity and the effect of ouabain in WT, TSC1-KO and TSC2-KO in MEF cells

After studying NKP activity in WT, TSC1-KO, and TSC2-KO MEFs and determining the optimal ouabain concentration for Rb^+ influx and K_i content, which was found to be 2 mM, the next step was to assess the impact of absence of the TSC1 and TSC2 genes and deregulation of the mTOR pathway could have on NKCC activity in these cells. The approach followed was similar to the studies with ouabain and consisted of determining the same parameters for bumetanide, i.e. BS_{max} and BIC_{50} for Rb^+ influx and K_i content at different ouabain concentrations, 0, 0.1 and 2 mM, to learn whether there were also abnormalities for bumetanide inhibition in the mutant cells as those found for ouabain.

Figure 11 shows the bumetanide dose-response of Rb^+ influx as a function of bumetanide (0-50 µM) at different ouabain concentrations (0, 0.1, 2 mM) in WT MEFs. Rb^+ influx followed a hyperbolic function with no statistically different values for the three ouabain concentrations tested in the absence of bumetanide whereas at increasing concentrations of the inhibitor a trend for lower Rb^+ influx values can be observed when ouabain increases from 0-2 mM. In spite of the differences between the bumetanide-dose response curves, saturation occurs at 20 µM bumetanide for the three cell types. Further analysis of the data, represented as the averages of Rb^+ influx for each of the curves, is shown in Figure 12. Results show a tendency for the averages to decrease with increasing ouabain concentrations although not statistically significant due to the large dispersion of the data.

The effect of ouabain on the dose-response of K_i content to increasing doses of bumetanide (0-50) and on their averages are shown in Figures 13 and 14, respectively. Neither the K_i content nor its averages were affected by bumetanide and ouabain in WT cells suggesting that outward K^+ movements occur through neither NKP nor NKCC under the experimental conditions tested.

a) Determination of the optimal bumetanide concentration for Rb^+ influx and K_i content in WT cells.

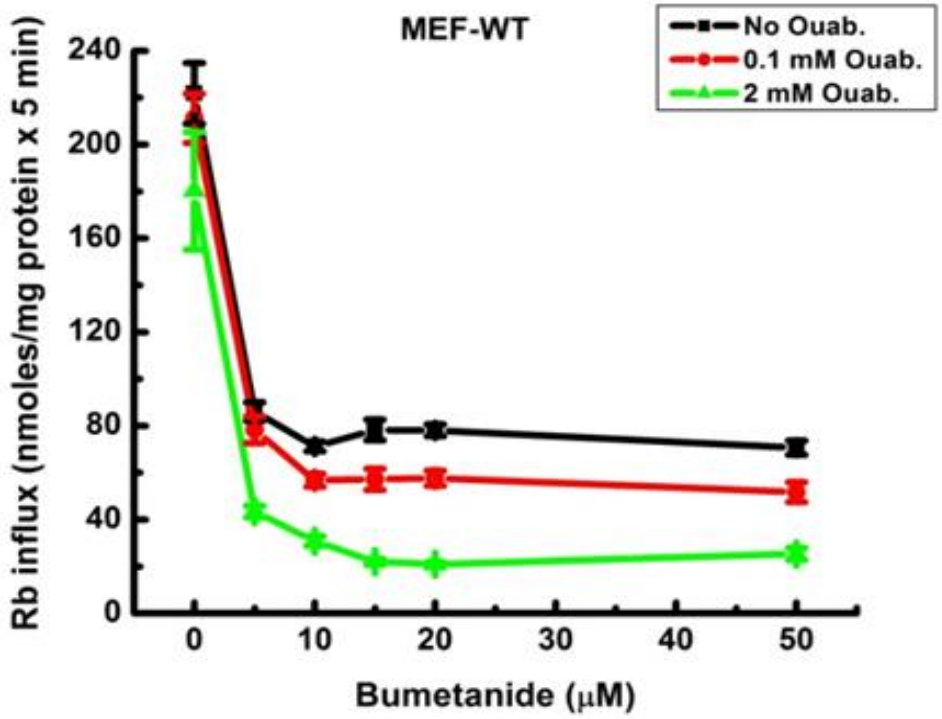

Figure 11 – Bumetanide dose-response (BDR) of Rb^+ influx in WT MEF cells and the effect of ouabain. Rb^+ influx was determined as described in Materials and Methods as a function of bumetanide (0-50 μM), and at three different ouabain concentrations (0, 0.1 and 2 mM). Flux time, 5 min. Number of individual determinations for WT MEF cells was n = 4. Values are means ± S.E. Details are discussed in the text.

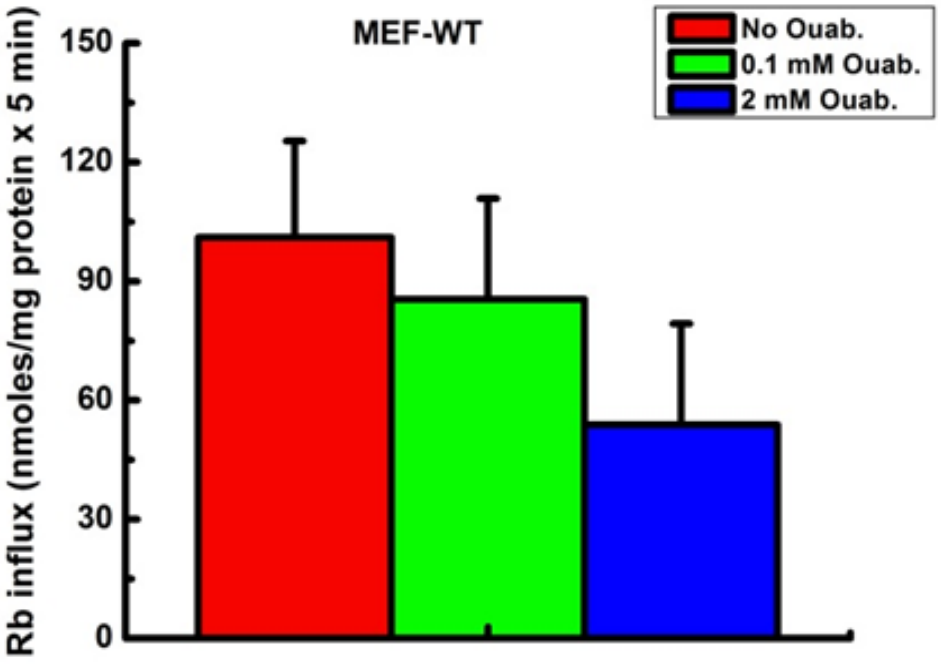

Figure 12 – Rb^+ influx averages from bumetanide dose-response of Rb^+ influx in WT MEF cells and the effect of ouabain. Rb^+ influx was determined as described in Materials and Methods. The Rb^+ influx averages were calculated from BDR curves in Figure 11 for each ouabain concentration and plotted as shown. Flux time, 5 min. Number of individual determinations for WT MEF cells was n = 4. Values are means ± S.E. Details are discussed in the text.

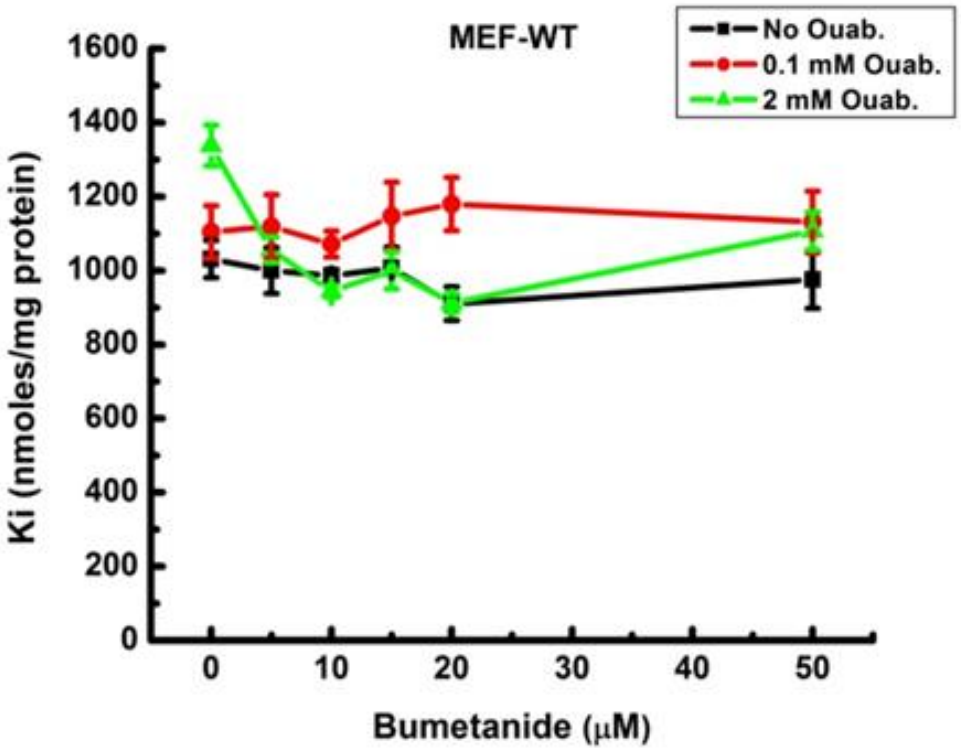

Figure 13 - Bumetanide dose-response of K_i content in WT MEF cells and the effect of ouabain. K_i content was determined after 5 min of incubation in the corresponding flux media, as described in Materials and Methods, as a function of bumetanide (0-50 μM), and at three different ouabain concentrations (0, 0.1 and 2 mM). Number of individual determinations for WT MEF cells was n = 4. Values are means ± S.E. Details are discussed in the text.

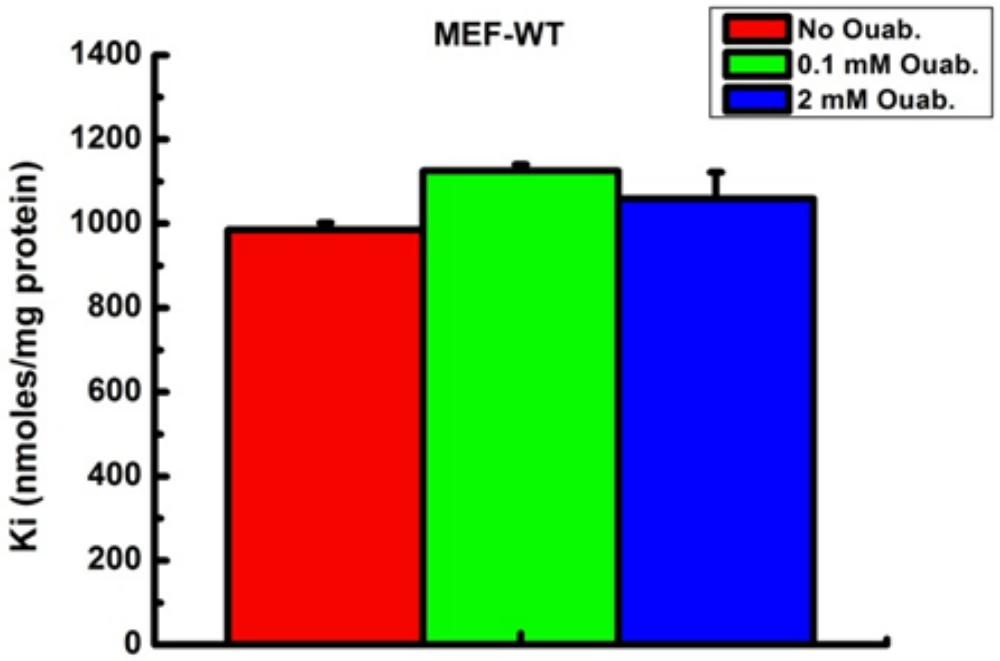

Figure 14 – K_i content averages from bumetanide dose-response of K_i content in WT MEF cells and the effect of ouabain. K_i content was determined as described in Materials and Methods. K_i content averages at 5 min were calculated from BDR curves in Figure 13 for each ouabain concentration and plotted as shown. Number of individual determinations for WT MEF cells was n = 4. Values are means ± S.E. Details are discussed in the text.

Like for ouabain, the maximal bumetanide inhibitory concentration (BS_{max}) was determined from the bumetanide-sensitive Rb^+ influx (NKCC activity) as a function of bumetanide in WT cells at 0, 0.1, and 2 mM ouabain (Figure 15). As it should be expected, NKCC activity was not affected by different ouabain concentrations, and likewise the half

maximal bumetanide inhibitory concentration (BIC_{50}) was not affected as shown in Figure 16.

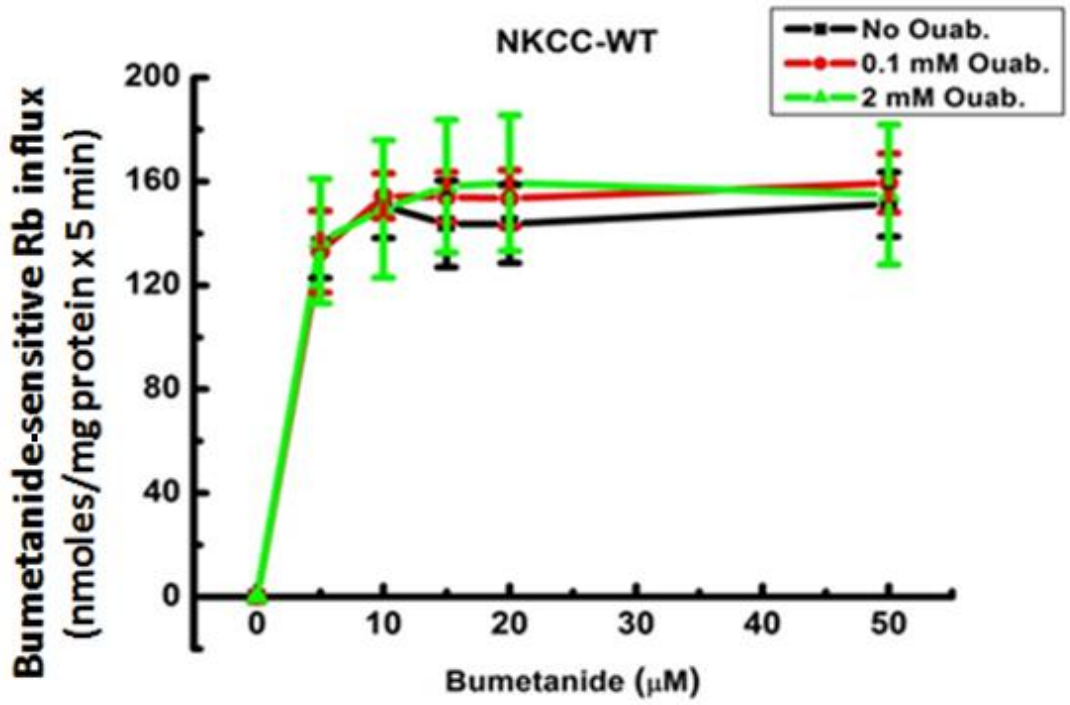

Figure 15 - Determination of the maximal bumetanide inhibitory concentration (BS_{max}) in WT MEF cells and the effect of ouabain. Rb^+ influx was determined as described in Materials and Methods and the bumetanide-sensitive (BS) fluxes were calculated from BDR curves (see Figure 11) for each bumetanide concentration. The BS_{max} was determined as the bumetanide dose at which saturation was reached. Flux time, 5 min. Number of individual determinations for WT MEF cells was n = 4. Values are means ± S.E. Details are discussed in the text.

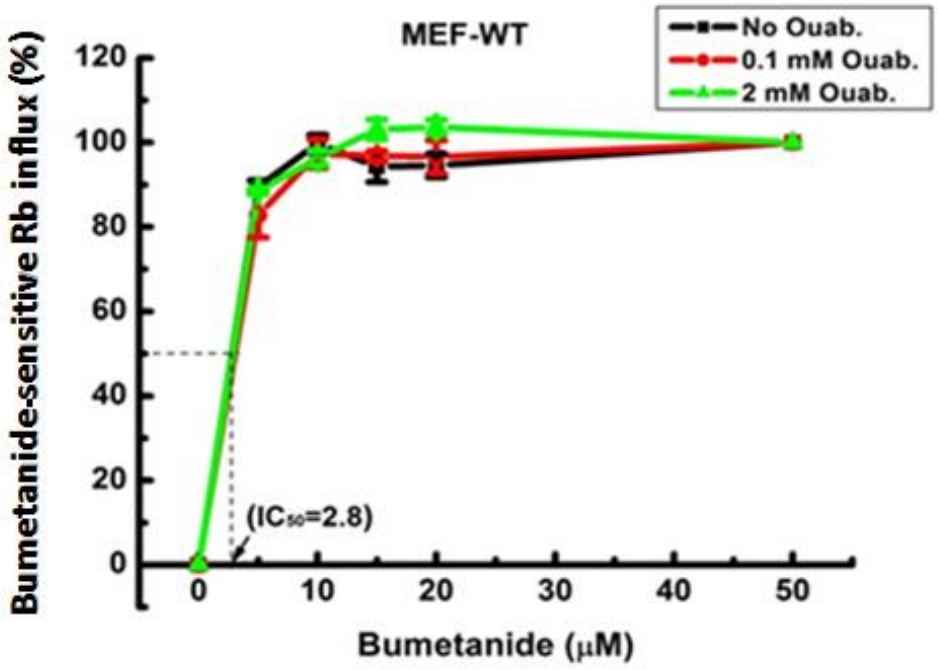

Figure 16 - Determination of the half maximal bumetanide inhibitory concentration (BIC_{50}) in WT MEF cells and the effect of ouabain. Rb^+ influx was determined as described in Materials and Methods and the bumetanide-sensitive (BS) fluxes were calculated from BDR curves (see Figure 11) for each bumetanide concentration. The bumetanide-sensitive Rb^+ influxes were calculated as percent of BS_{max}, which was assigned arbitrarily a 100 % value for all curves. The BIC_{50} values were obtained from the fitted curve at the 50 % value. Flux time was 5 min. Number of individual determinations (n) for WT MEF cells was n = 4. Values are means ± S.E. Details are discussed in the text.

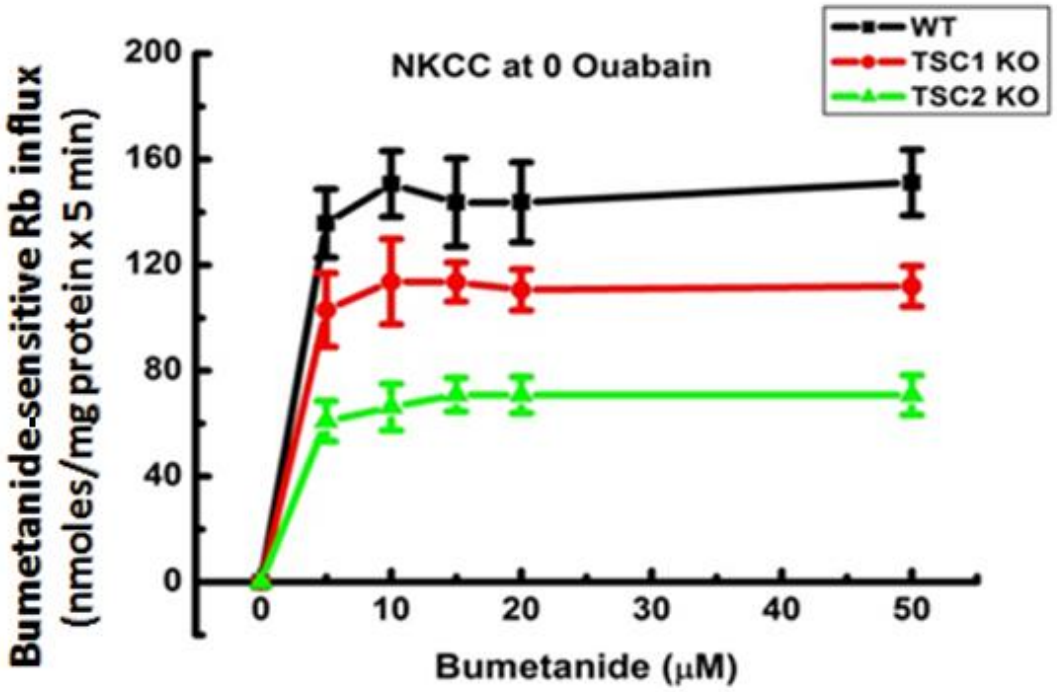

Figure 17 - Comparison of BS_{max} for WT, TSC1-KO, and TSC2-KO at zero ouabain. Rb^+ influx was determined as described in Materials and Methods for each cell type in the absence of ouabain and the bumetanide-sensitive (BS) fluxes were calculated from BDR curves (see Figure 11) for each bumetanide concentration. The BS_{max} was determined as the bumetanide dose at which saturation was reached. Flux time was 5 min. Number of individual determinations for WT, TSC1-KO and TSC2-KO MEF cells were n = 4, 6 and 10, respectively. Values are means ± S.E. Details are discussed in the text.

The same approach followed for WT cells was applied to TSC1-KO and TSC2-KO MEF cells to determine BS_{max} and BIC_{50} at each ouabain concentration to assess whether there was any interaction between bumetanide and ouabain while inhibiting NKCC. Figures

17 and 18 show the bumetanide-sensitive Rb^+ influx (NKCC) as a function of bumetanide for each of the three cell types, either at 0 or 2 mM ouabain, respectively, where the BS_{max} can be appreciated. Unexpectedly and in contrast to what was found for WT cells, BS_{max} values for the mutants were significantly lower at both 0 and 2 mM ouabain. The sequence found was WT > TSC1-KO > TSC2-KO, where the decrease for TSC1-KO and TSC2-KO was about 30 % and 50 %, and 50 % and 75 % at 0 and 2 mM ouabain, respectively, compared to WT. A plausible explanation for this unexpected result will be given in the Discussion.

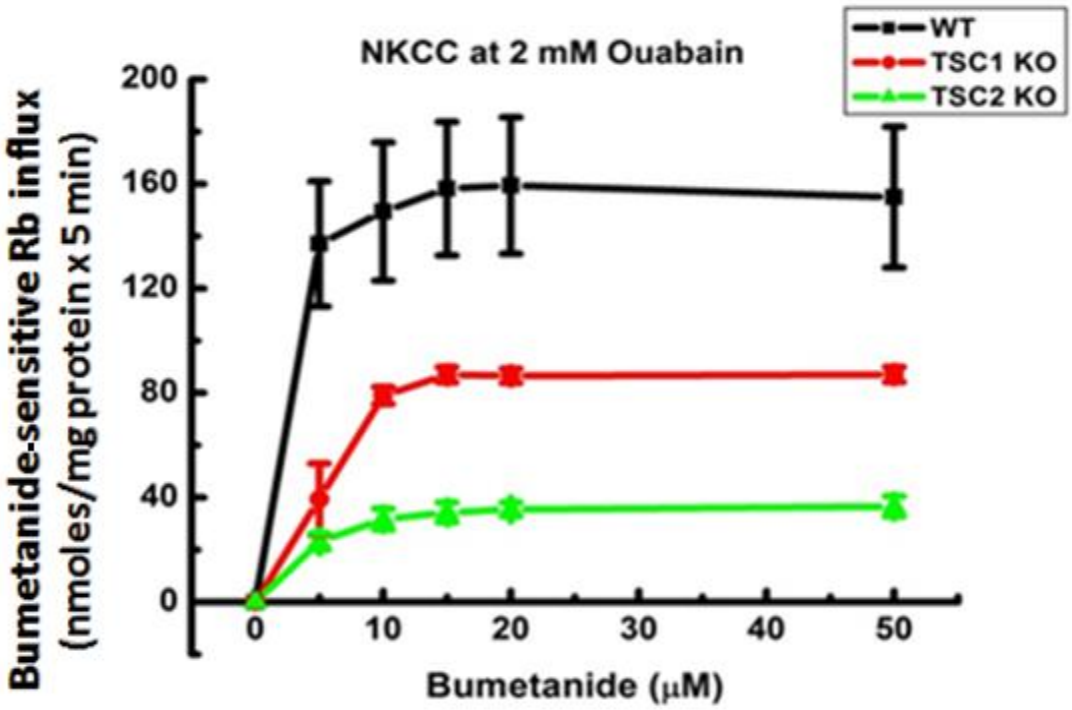

Figure 18 - Comparison of BS_{max} for WT, TSC1-KO, and TSC2-KO at 2 mM ouabain. Rb^+ influx was determined as described in Materials and Methods for each cell type at 2 mM ouabain and the bumetanide-sensitive (BS) fluxes were calculated from BDR curves (see Figure 11) for each bumetanide concentration. The BS_{max} was determined as the bumetanide dose at which saturation was reached. Flux time was 5 min. Number of individual determinations (n) for WT, TSC1-KO and TSC2-KO MEF cells were n = 4, 6 and 10, respectively. Values are means ± S.E. Details are discussed in the text.

Thus TSC2-KO cells showed larger changes than those of TSC1-KO for all the parameters determined, and especially, for the activity of bumetanide=sensitive Rb^+ influx (NKCC) which was significantly reduced when compared not only to WT but also to TSC1-KO cells (Figures 17 and 18).

A summary of bumetanide effects on Rb^+ influx in WT, TSC1-KO and TSC2-KO MEF cells and the effect of ouabain is shown in Table 3.

b) Summary of bumetanide-dose-response of Rb^+ Influx, IC_{50} and BS_{max} in WT, TSC1-KO and TSC2-KO MEF cells and the effect of ouabain.

Half maximal bumetanide inhibitory concentration (BIC_{50}) and maximal bumetanide-sensitive Rb^+ influx (BS_{max}) at 0, 0.1, and 2 mM ouabain for WT, TSC1-KO, and TSC2-KO cells are summarized in Table 3 in order to see if there is a difference in

these parameters between the three cell types. BIC_{50} is is expressed in µM and BS_{max} in nmol/mg protein.

Cells	WT			TSC1-KO			TSC2-KO		
Ouab.	0	0.1	2	0	0.1	2	0	0.1	2
BIC_{50}	2.8	2.8	2.8	2.9	2.9	5.7	2.1	4.3	2.8
SE	-	-	-	0.6	0.85	2.2	0.4	2.6	1.2
SD	-	-	-	0.8	1.2	3.1	0.6	3.7	1.6
BS_{max}	151	159	157	112	103	87*	71	37*	34**
SE	-	-	-	15.4	34.6	1.2	2.9	14	6.8
SD	-	-	-	21.8	49	1.7	4.1	120	9.7
n	4	4	4	6	6	6	10	10	10
N	1	1	1	2	2	2	4	4	4

Table 3 - Maximal bumetanide-sensitive (BS_{max}) Rb^+ influx and half maximal bumetanide inhibitory concentration (BIC_{50}), statistical parameters and number of individual determinations (n) and independent experiments (N) performed for WT, TSC1-KO, and TSC2-KO cells at different ouabain concentrations (0, 0.1 and 2 mM).

Table 3 shows the BIC_{50} and BS_{max} for WT, TSC1-KO, and TSC2-KO MEF cells at 0, 0.1, and 2 mM ouabain. The BIC_{50} for the three cell types was not statistically different

with increasing ouabain between 0 to 2 mM, whereas the BS_{max} did show statistically significant differences for the effect of ouabain in a given cell type or between cell types at a given ouabain concentration. Thus, in WT, ouabain had no effect on BS_{max}, in contrast to the mutants where increasing ouabain was associated with decreasing BS_{max}. Larger changes were observed for TSC2-KO compared to TSC1-KO cells. In addition, the magnitude of the BS_{max} values followed the sequence WT > TSC1-KO > TSC2-KO, which resembles the trend observed for most of the variables determined in this study and where absence of the TSC2 gene appears to cause a more abnormal deregulation of the mTOR pathway than the absence of TSC1 [3, 53, 55, 56].

One of the aims of this study was to assess the relative activities of the main pathways for K^+ transport that are known to be involved in cell volume regulation, migration and proliferation. These are NKP, NKCC and KCC. Another purpose was oto assess whether murine embryonic fibroblasts behave as adult cells in terms of their ion transport properties and to understand which of the two genes, TSC1 or TSC2, have a major impact if any on K^+ homeostasis as determined by Rb^+ influx and K_i content. The studies described above were designed to provide the optimal ouabain and bumetanide concentrations for the three cell types, WT, TSC1-KO and TSC2-KO MEF cells to accomplish this goal. The conclusion from such studies is that 2 mM ouabain and 20 μM bumetanide were the optimal concentrations to further assess the activity of the aforementioned pathways under more physiological conditions.

Figure 19 shows the Rb^+ influx pathways measured at optimal ouabain (2 mM) and bumetanide concentrations (20 μM) for WT, TSC1-KO and TSC2-KO MEF cells. Rb^+ influx was determined as described in Materials and Methods in the presence and absence of Cl^-, ouabain and bumetanide to determine the activities of NKP, NKCC and KCC. In the upper panel, the Rb^+ influx was measured in chloride (Cl), chloride + 2 mM ouabain (ClO), chloride + 2 mM ouabain + 20 μM bumetanide (ClOB) and sulfamate + 2 mM ouabain + 20 μM bumetanide (SOB). In the lower panel, the calculated NKP, NKCC and KCC activities are represented for each cell type. It is clear from the figure that the major difference for all the variables studied appears in TSC2-KO cells where Rb^+ influx in all the media, ± Cl^- and ± inhibitors, and through the three transporters in question is significantly diminished when compared to both WT and TSC1-KO. For the latter, the only difference observed was a decrease in ClOB and consequently, a decrease in KCC. However, the NKCC activity, although elevated was not statistically different from that in WT cells. In these cells, NKP and NKCC contributed to 92 % of the total Rb^+ influx whereas only 8 % of the influx occurred through KCC. The major contributor for Rb^+ influx in WT cells was NKCC (68 %) followed by NKP (24 %) and KCC (8%).

According to the hypothesis tested in this study, TSC1-KO and TSC2-KO MEF cells should have increased mTORC1 activity [44]. Increased mTORC1 activity affects the activity of NKCC as shown in mammalian skeletal muscle cells [41, 42, 44] and the expression of KCC as shown in human cells [43, 44]. In fact, the baseline NKCC activity in TSC1-KO cells was 90 % of the total Rb^+ influx followed by NKP (5 %) and KCC (5 %), in contrast to the values observed in WT cells. However, the total Rb^+ influx through

NKP, NKCC, and KCC in WT and TSC1-KO cells was the same, whereas that of TSC2-KO was less than 40 % when compared to WT and TSC1-KO and shown in [Fig.19].

In conclusion, these findings are in agreement with studies on the effect of deregulation of the mTOR pathway on NKCC activity and KCC expression [41, 42, 43], and will be further analyzed in the Discussion.

4.4. Rb^+ influx and K_i content in WT, TSC1-KO and TSC2-KO in MEF cells.

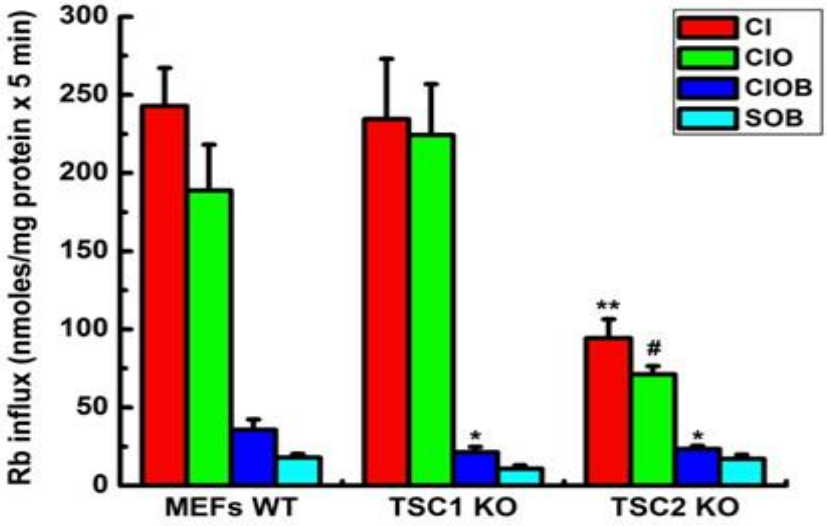

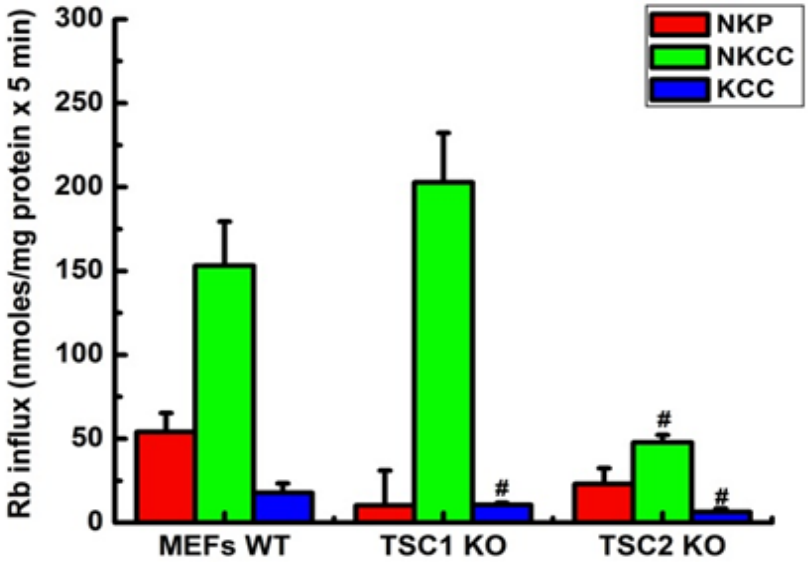

Figure 19 – Rb^+ influx pathways at optimal ouabain and bumetanide concentrations for WT, TSC1-KO and TSC2-KO MEF cells. Rb^+ influx was determined as described in Materials and Methods in the presence and absence of Cl^-, ouabain and bumetanide to determine the activities of NKP, NKCC and KCC at optimal inhibitor concentrations, 2 mM ouabain and 20 uM bumetanide. Upper panel: Cl, ClO, ClOB and SOB. Lower panel: NKP, NKCC and KCC for each cell type. Flux time was 5 min and Rb^+ influx components and transporters were calculated as described in Materials and Methods. Number of individual determinations (n) for WT, TSC1-KO and TSC2-KO MEF cells were n = 12, 6 and 12, respectively. Values are means ± S.E. Details are discussed in the text.

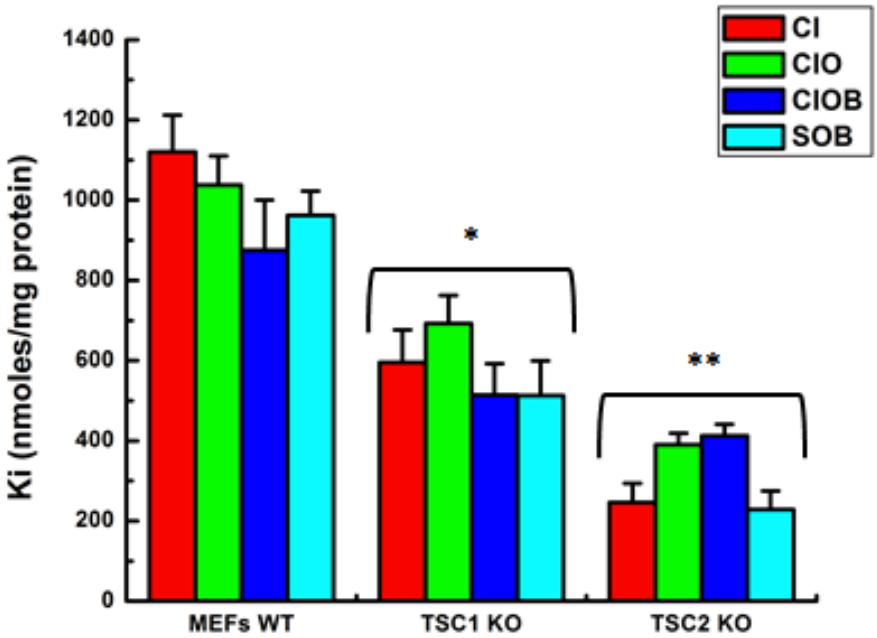

Figure 20: K_i content at optimal ouabain and bumetanide concentrations for WT, TSC1-KO and TSC2-KO MEF cells. K_i content was determined as described in Materials and Methods in the presence and absence of Cl^-, ouabain and bumetanide at optimal inhibitor concentrations, 2 mM ouabain and 20 μM bumetanide in the corresponding media: Cl, ClO, ClOB and SOB for each cell type. Flux time was 5 min. Number of individual determinations for WT, TSC1-KO and TSC2-KO MEF cells were n = 12, 6 and 12, respectively. Values are means ± S.E. Details are discussed in the text.

Figure 20 shows K_i content in WT, TSC1-KO and TSC2-KO MEF cells under the same conditions as described in Figure 19. In the mutant cells, K_i content was surprisingly low (~40 % in TSC1-KO and ~60 % in TSC2-KO lower compared to WT cells). The loss of K^+ occurs through none of the transporters studied, as shown in the figure, and may be lost perhaps through an unidentified K^+ channel that requires further exploration.

4.5. Proposed model of the factors affecting K_i homeostasis in TSC1-KO and TSC2-KO MEFs.

According to our hypothesis, when the TSC1 gene in MEF cells is mutated or knocked out, the mTORC1 activity increases [3-6] and consequently affects NKCC activity and KCC expression [3 - 6, 41 - 43]. As a result, highly active mTORC1 causes activation of NKCC and inhibition of KCC [4 - 6].

This model explains the effect of the TSC1 and TSC2 genes on K^+ homeostasis through the mTOR pathway in MEF cells. In the upper panel, the mutated TSC1 gene

increases mTORC1 activity and it may decrease NKP activity (Table 2 and Figs. 9 and 19). A decrease in NKP activity may be explained by consumption of ATP by mTORC1. ATP is needed in the NKP cycle to transport Na^+ and K^+, [44 - 47]. NKCC and KCC activities were statistically significantly increased and decreased, respectively, in TSC1-KO cells due to the effect of a highly active mTORC1 (Figs. 19 and 20). Lastly, the total magnitude of Rb^+ (K^+) influx through the three pathways was similar to that found in WT cells (Fig. 19) see the upper panel of (Fig. 21).

On the other hand, as shown in the lower panel of this model, a mutated TSC2 gene increases the mTORC1 activity, as it occurs in TSC1-KO cells, and it may decrease the NKP activity (Table 2 and Figs. 9 and 19), as seen in TSC1-KO cells (Figs. 19 and 20). However, the striking difference between the two mutants is the low magnitude of Rb^+ (K^+) influx and K_i content in TSC2-KO cells (Figs. 4 – 9, Table 2 and 3) compared to WT and TSC1-KO cells (Figs. 19, 20).

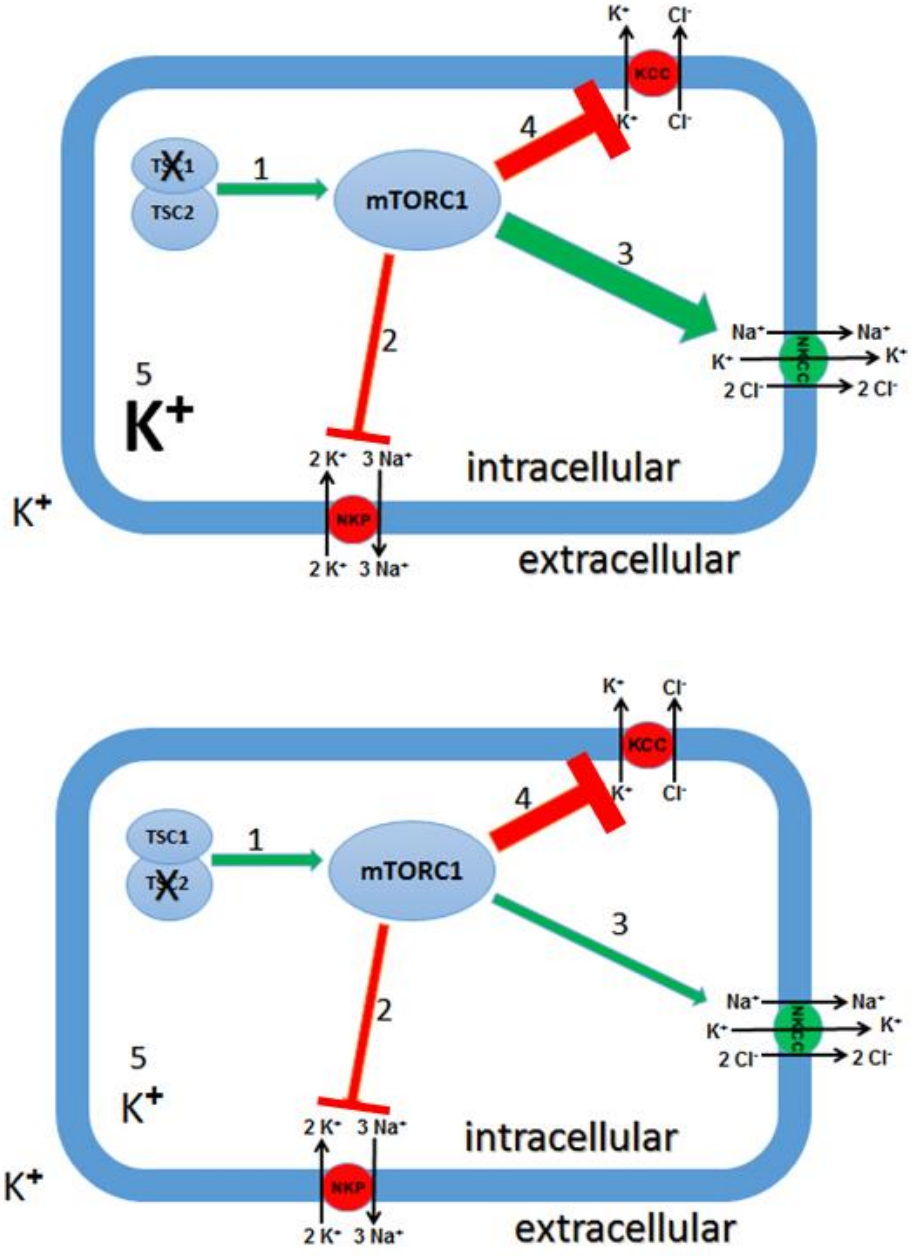

Figure 21. Hypothetical model of the factors affecting K_i homeostasis in TSC1-KO and TSC2-KO MEFs. 1 = activation of mTORC1 as a result of mutation in the TSC1 or TSC2 genes. Higher activity of mTORC1 causes 2 = less NKP activity, 3 = activation of NKCC, and 4 = less expression of KCC. Big K^+ means higher

intracellular potassium in TSC1-KO cells (upper panel). Small K^+ means lower intracellular potassium in TSC2-KO cells (lower panel).

5. Discussion

The TSC1-TSC2 complex plays a crucial role in the inhibition of mTORC1 and activation of mTORC2, and ultimately in the regulation of NKCC activity and KCC expression through a negative feedback process involving S6K1, Akt, IGF-1, and several other proteins [4, 5, 6, 41, 42, 43] because mTORC1 phosphorylates S6K1, while (mTORC2) phosphorylates Akt [3, 5]. Highly active S6K1 causes feedback inhibition of IRS-1 leads to inability of insulin or IGF1 to activate PI3K and subsequently Akt [3, 4, 5, 25].

The present study investigated the role of the TSC1 and TSC2 genes, and indirectly, of the mTOR pathway on cellular K^+ homeostasis in WT, TSC1-KO, and TSC2-KO MEF cells. The approach was to measure Rb^+ influx and K_i content to assess the impact of these genes on the K^+ transporters, NKP, NKCC and KCC, known to be involved in K^+ homeostasis, cell volume regulation, proliferation, migration and in other cellular metabolic processes [1, 32, 43, 51, 58]. Our main findings show that in MEF cells overall, the activities of the transporters studied followed the sequence NKCC > NKP > KCC, which resemble findings in adult murine cells. However, there were differences in their relative magnitudes within and across cell types. For instance, in the mutants, the activities of NKP and KCC were statistically lower than in WT cells whereas NKCC was 25 % greater in

TSC1-KO than in WT, and in TSC2-KO cells, where it was about 70 % lower than for both WT and TSC1-KO cells (Fig.19).

The decreased NKP activity in knockout cells, about 50% less than in WT cells (Table 2 and Figs. 9 and 19), may be explained by extensive consumption of ATP, which is needed in the NKP cycle to transport Na^+ and K^+, by mTORC1. As a matter of fact, TSC1-KO and TSC2-KO cells are considered models of increased mTORC1 activity [44, 45, 46, 47]. However, the averages of Rb^+ influx and K_i content in TSC2-KO cells are considerably less than in TSC1-KO and WT cells. A plausible explanation may lie on the magnitude of NKCC activity in TSC1-KO compared to TSC2-KO which can transport Rb^+ (K^+) inward or outward depending on the gradient. Further studies on NKCC and KCC are needed to address this particular point.

The mTORC1 activity is increased in cells lacking either the TSC1 (hamartin) and/or TSC2 (tuberin) genes, which in turn affect the activity of NKCC and the expression of KCC [41, 43, 44], through a negative feedback inhibition of insulin receptor substrate 1 (IRS-1), as shown in mammalian skeletal muscle and human cells. Therefore, the mTORC1-driven feedback inhibition of IRS-1 prevents insulin or IGF1 to activate PI3K and subsequently Akt [41 - 43, 45]. Thus, defects in the TSC1-TSC2 complex activate mTORC1 and S6K1 constitutively. This activation of S6K1 hyper phosphorylates and degrades IRS-1. As a result of the IRS-1 degradation, the PI3K signaling will be attenuated. PI3K affects the phosphorylation of Akt, so expression of KCC will be decreased and activity of NKCC will be increased [41 - 43, 45] because KCC expression and NKCC

activity are dependent on Akt in opposite ways which means when Akt is attenuated, KCC expression decreases and NKCC activity increases.

In our results the baseline NKCC activity was 90 % of the total Rb^+ influx, followed by NKP (5 %) and KCC (5 %) in TSC1-KO cells as shown in (fig. 19), in contrast to the values observed in WT cells These findings are in agreement with reports in mammalian skeletal muscle and human cells where the activities of NKCC and KCC were increased and decreased, respectively, in cells lacking the TSC1 and TSC2 genes. Likewise, in TSC2-KO cells, albeit possessing lower NKCC and KCC activities than in TSC1-KO cells, NKCC was the predominant pathway, whereas KCC was the minor route for K^+ movements (Fig. 19), fulfilling the predictions of our hypothesis.

According to various studies on the affinity of ouabain for NKP in human cells (HEK293), the concentrations of ouabain to inhibit NKP are in the µM range (~ 0.1 mM) [57, 58]. However, in mouse cells, the concentrations are in the mM range (~ 1 mM) [59]. In our studies, in order to determine the optimal ouabain concentration to inhibit NKP in MEF cells, we have done ouabain dose-response (ODR) curves for Rb^+ influx [Figures 5 and 6] and K_i content [Figures 7 and 8] and we found that the OIC_{50} was ~ 0.5 mM for both WT and mutant cells and OS_{max} was around 121 nmoles/mg protein for WT cells, but for the mutants cells the OS_{max} was ~ 60 nmoles/mg protein (Table 2). Thus, the optimal ouabain concentration in these cells was 2 mM [Figures 5 and 9].

Therefore, the relative values of Rb^+ influx followed the sequence WT > TSC1-KO > TSC2-KO at 0 mM ouabain, whereas that of the mean values obtained by averaging the

Rb^+ influx from the ODR curves for each cell type was WT ~ TSC1-KO > TSC2-KO [Figures 6 and 8]. In addition, there was no difference in the OIC_{50s} (~ 0.5 mM) (Table 2) and for the OS_{max} the sequence was WT > TSC1-KO ~ TSC2-KO (Table 2). As a conclusion, ouabain binds with low affinity to NKP in MEF cells compared to human erythrocytes (IC_{50} ~ 4 x 10^{-8} M) [66]. Our results are also in agreement with findings in adult murine cells.

On the other hand, the bumetanide concentrations to block NKCC in primary rat neurons cells are in the µM range. For instance, at ~ 10 µM there is strong inhibition of NKCC [60]. However, in our studies with MEF cells, the actual values were not known. Thus, to determine the optimal bumetanide concentration, we have done bumetanide dose-response (BDR) curves for Rb^+ influx [Figures 11 and 12] and K_i content [Figures 13 and 14] and found that 20 µM bumetanide was the optimal concentration to maximally inhibit NKCC at 0, 0.1, and 2 mM ouabain in the three cell types [Figs. 11, 15, 17, and 18]. In addition, we determined the maximal bumetanide-sensitive Rb^+ influx (BS_{max}) and the half maximal bumetanide inhibitory concentration (BIC_{50}) at different ouabain concentrations [Figs. 15 - 18]. The relative values of Rb^+ influx followed the sequence WT > TSC1-KO > TSC2-KO at 0, 0.1, and 2 mM ouabain whereas that of the mean values obtained by averaging the Rb^+ influx from the ODR curves for each cell type was WT > TSC1-KO > TSC2-KO at 0, 0.1, and 2 mM ouabain. In conclusion, while ouabain did not affect the BIC_{50} as a function of its concentration for the three cell types (~ 3 µM), it did affect the maximal activity of NKCC both as a function of ouabain concentration in the mutants and

in TSC2-KO more than in TSC1-KO, but not in WT cells (figures 17 and 18 and Table 3). Also, mouse cells needs slightly more bumetanide concentration (20 µM) to inhibit NKCC comparing to rat neuron cells (10 µM) which means that MEF cells have merely less affinity for bumetanide compared to rat cells [60].

In conclusion, the major findings in this study support the hypothesis proposing that the TSC1 and TSC2 genes, which control cell processes through the mTOR pathway, are important for K^+ homeostasis where the activities of NKP were reduced, NKCC increased and KCC decreased, according to expectations and the proposed model (figures 21). Furthermore, cells lacking the TSC2 gene showed more striking changes concerning K^+ homeostasis than those seen in cells lacking the TSC1 gene (Figures; 4, 6, 8, 17, 18, 19, 20, and Tables 2 and 3). Furthermore, the distinct abnormalities in ion transport of TSC2-KO compared to TSC1-KO and WT cells parallels the pathological manifestation and incidence of tuberous sclerosis complex in the human population [3, 53, 54, 55, 56].

6. Acknowledgements

I am deeply thankful to Dr. Norma C Adragna and Dr. Peter K Lauf for giving me the opportunity to be a member of the Cell Biophysics laboratory and for providing excellent atmosphere and providing all the resources related to my project. I am very grateful for their guidance and critical readings of the manuscript. In addition, I am grateful to Dr. Kristopher T Kahle for providing us the MEFs cell lines (WT, TSC1-KO, and TSC2-KO). I wanted also to thank Dr. Jeffrey B. Travers, M.D., Ph.D, for being in my committee. I acknowledge gratefully Mr. Nagendra Ravilla for providing me excellent training with cell cultures and flux studies including working with Atomic Absorption Spectroscopy. I am also thankful to my colleagues in the Cell Biophysics laboratory, Department of Pharmacology and Toxicology, and my family and friends for their support.

I would like also to thank my parents for supporting me all way from the day I was born till now and I also would like to thank the King Abdullah Scholarship Program for giving me the opportunity to be part of this program, trying to equip students with knowledge and skills to be future world leaders, and most importantly giving me the chance to proceed my educational dreams, a Master's degree in Pharmacology and Toxicology, I had always thought of. Furthermore, I thank my lovely country Kingdom of Saudi Arabia (KSA) for giving me the opportunity to study in the USA. Finally, I thank God for making this progress in my life happen and I say "thanks God" for everything.

Abbreviations:

AMPK, AMP-activated kinase which is an enzyme that plays a role in cellular energy homeostasis; 4E-BP, eIF4E binding protein is a protein that play an important role in the control of protein synthesis, survival, and cell growth, eIF4E, eukaryotic initiation factor 4E is a cap-binding protein that participates in recruitment of mRNA to the ribosome; Mnk1, mitogen-activated protein kinase-interacting kinase 1; mTORC1, mammalian target of rapamycin complex 1; mTORC2, mammalian target of rapamycin complex 2; PDK1, phosphoinositide-dependent protein kinase 1; PtdIns(3,4,5)P3, phosphatidylinositol-3,4,5-triphosphate; PtdIns(4,5)P2, phosphatidylinositol-4,5-bisphosphate; raptor, regulatory associated protein of tor; rictor, rapamycin-insensitive companion of mtor; S6, ribosomal protein S6; S6K, p70S6 kinase; S473, serine 473; T308, threonine 308; TSC, tuberous sclerosis complex; RVD, regulatory volume decrease; RVI, regulatory volume increase; NKP, Na^+/K^+ pump; NKCC, Na^+-K^+-$2Cl^-$ co-transporter; KCC, K-Cl cotransport; mTOR, mammalian target of rapamycin; TSC1, tuberous sclerosis complex 1; TSC2, tuberous sclerosis complex 2; MEFs, mouse embryonic fibroblasts; MEFs WT, mouse embryonic fibroblasts wild type; MEFs TSC1-KO, mouse embryonic fibroblasts-tuberous sclerosis complex 1 knockout; MEFs TSC2-KO, mouse embryonic fibroblasts-tuberous sclerosis complex 2 knockout; CDK1, cyclin-dependent kinase 1; GSK3β, glycogen synthase 3β; ERK2, extra cellular related kinase 2; MK2, mitogen-activated protein kinase–activated protein kinase 2; AKT/PKB, protein kinase b; RSK1, p90 ribosomal s6 kinase 1; GAP, GTP-ase activating protein; PI3K, phosphatidylinositol-4,5-bisphosphate 3-kinase; AICAR, 5-amino-4-imidazolecarboxamide ribose; Rheb, RAS homolog enriched in brain; FRAP1, fk506-binding protein 12-rapamycin-associated protein 1; mLST8, mammalian lethal with

sec13 protein 8; mSIN1, mammalian stress-activated protein kinase (sapk)-interacting protein 1; FKBP12, FK506 binding protein; FRB, FKBP12-rapamycin binding; IGF-1, insulin-like growth factor 1; IGF-2, insulin-like growth factor 2; S6K1, ribosomal protein s6 kinase beta-1; ROS, reactive oxygen species; ATP, adenosine triphosphate; slc12a2, solute carrier family 12 (sodium/potassium/chloride transporter), member 2; slc12a1, solute carrier family 12 (sodium/potassium/chloride transporter), member 1; PKC, protein kinase c; PKA, protein kinase a; CNS, central nervous system.

7. References

1. Lang, F., Cell volume regulation. Contributions to nephrology. 1998, Basel; New York: Karger. vii, 264 p.
2. Mongin, A.A. and S.N. Orlov, Mechanisms of cell volume regulation and possible nature of the cell volume sensor. Pathophysiology, 2001. 8(2): p. 77-88.
3. Crino, P.B., K.L. Nathanson, and E.P. Henske, The tuberous sclerosis complex. N Engl J Med, 2006. 355(13): p. 1345-56.
4. Huang, J. and B.D. Manning, A complex interplay between Akt, TSC2 and the two mTOR complexes. Biochem Soc Trans, 2009. 37(Pt 1): p. 217-22.
5. Huang, J., et al., The TSC1-TSC2 complex is required for proper activation of mTOR complex 2. Mol Cell Biol, 2008. 28(12): p. 4104-15.
6. Buchkovich, N.J., et al., The TORrid affairs of viruses: effects of mammalian DNA viruses on the PI3K-Akt-mTOR signaling pathway. Nat Rev Microbiol, 2008. 6(4): p. 266-75.
7. Manning, B.D., et al., Identification of the tuberous sclerosis complex-2 tumor suppressor gene product tuberin as a target of the phosphoinositide 3-kinase/akt pathway. Mol Cell, 2002. 10(1): p. 151-62.
8. Huang, J. and B.D. Manning, The TSC1-TSC2 complex: a molecular switchboard Controlling cell growth. Biochem J, 2008. 412(2): p. 179-90.
9. Inoki, K., et al., Rheb GTPase is a direct target of TSC2 GAP activity and regulates mTOR signaling. Genes Dev, 2003. 17(15): p. 1829-34.
10. Benvenuto, G., et al., The tuberous sclerosis-1 (TSC1) gene product hamartin suppresses cell growth and augments the expression of the TSC2 product tuberin by inhibiting its ubiquitination. Oncogene, 2000. 19(54): p. 6306-16.

11. Inoki, K., T. Zhu, and K.L. Guan, TSC2 mediates cellular energy response to control cell growth and survival. Cell, 2003. 115(5): p. 577-90.
12. Hay, N. and N. Sonenberg, Upstream and downstream of mTOR. Genes Dev, 2004. 18(16): p. 1926-45.
13. Betz, C. and M.N. Hall, Where is mTOR and what is it doing there? J Cell Biol, 2013. 203(4): p. 563-74.
14. Sarbassov, D.D., et al., Rictor, a novel binding partner of mTOR, defines a rapamycininsensitive and raptor-independent pathway that regulates the cytoskeleton. Curr Biol, 2004. 14(14): p. 1296-302.
15. Betz, C., et al., Feature Article: mTOR complex 2-Akt signaling at mitochondria-associated endoplasmic reticulum membranes (MAM) regulates mitochondrial physiology. Proc Natl Acad Sci U S A, 2013. 110(31): p. 12526-34.
16. Sarbassov, D.D., et al., Phosphorylation and regulation of Akt/PKB by the rictor-mTOR complex. Science, 2005. 307(5712): p. 1098-101.
17. Stephens, L., et al., Protein kinase B kinases that mediate phosphatidylinositol 3,4,5trisphosphate-dependent activation of protein kinase B. Science, 1998. 279(5351): p. 710-4.
18. Lamming, D.W., et al., Rapamycin-induced insulin resistance is mediated by mTORC2 loss and uncoupled from longevity. Science, 2012. 335(6076): p. 1638-43.
19. Guyton, A.C. and J.E. Hall, Textbook of medical physiology. 11th ed. 2006, Philadelphia: Elsevier Saunders. xxxv, 1116 p.
20. Lang, F. and M. Fo\ller, Erythrocytes : physiology and pathophysiology. 2012, London: Imperial College Press.
21. Blanco, G. and R.W. Mercer, Isozymes of the Na-K-ATPase: heterogeneity in structure, diversity in function. Am J Physiol, 1998. 275(5 Pt 2): p. F633-50.

22. Hubner, C.A., D.E. Lorke, and I. Hermans-Borgmeyer, Expression of the Na-K-2Clcotransporter NKCC1 during mouse development. Mech Dev, 2001. 102(1-2): p. 267-9.

23. Haas, M., The Na-K-Cl cotransporters. Am J Physiol, 1994. 267(4 Pt 1): p. C869-85.

24. Smith, P.K., et al., Measurement of protein using bicinchoninic acid. Anal Biochem, 1985. 150(1): p. 76-85.

25. Zhang, J., P.K. Lauf, and N.C. Adragna, Platelet-derived growth factor regulates K-Cl cotransport in vascular smooth muscle cells. Am J Physiol Cell Physiol, 2003. 284(3): p. C674-80.

26. Adragna, N.C., et al., KCl cotransport regulation and protein kinase G in cultured vascular smooth muscle cells. J Membr Biol, 2002. 187(2): p. 157-65.

27. Adragna, N.C., Cation transport in vascular endothelial cells and aging. J Membr Biol, 1991. 124(3): p. 285-91.

28. Markadieu, N. and E. Delpire, Physiology and pathophysiology of SLC12A1/2 transporters. Pflugers Arch, 2014. 466(1): p. 91-105.

29. Mercado, A. and Z. Melo, [Pathophysiological aspects of K+: Cl- cotransporters]. Rev Invest Clin, 2014. 66(2): p. 173-80.

30. Kaila, K., et al., Cation-chloride cotransporters in neuronal development, plasticity and disease. Nat Rev Neurosci, 2014. 15(10): p. 637-54.

31. Orlov, S.N., et al., Cation-chloride cotransporters: regulation, physiological significance, and role in pathogenesis of arterial hypertension. Biochemistry (Mosc), 2014. 79(13): p. 154661.

32. Hoffmann, E.K., I.H. Lambert, and S.F. Pedersen, Physiology of cell volume regulation in vertebrates. Physiol Rev, 2009. 89(1): p. 193-277.

33. Chen, Y.-F., Chou, C.-Y., Ellory, J. C., & Shen, M.-R. (2010). the emerging role of KCl cotransport in tumor biology. American Journal of Translational Research, 2(4), 345–355.

34. Kahle, K.T., J. Rinehart, and R.P. Lifton, Phosphoregulation of the Na-K-2Cl and K-Cl cotransporters by the WNK kinases. Biochim Biophys Acta, 2010. 1802(12): p. 1150-8.

35. Lauf, P.K., K:Cl cotransport: emerging molecular aspects of a ouabain-resistant, volume-responsive transport system in red blood cells. Ren Physiol Biochem, 1988. 11(3-5): p. 248-59.

36. Payne, J. A. (1997). Functional characterization of the neuronal-specific K-Cl cotransporter: Implications for [K+]o regulation. The American Journal of Physiology, 273(5 Pt 1), C1516-25.

37. Lauf, P.K., et al., KCC2a expression in a human fetal lens epithelial cell line. Cell Physiol Biochem, 2012. 29(1-2): p. 303-12.

38. Chen, Y.-F., Chou, C.-Y., Ellory, J. C., & Shen, M.-R. (2010). the emerging role of KCl cotransport in tumor biology. American Journal of Translational Research, 2(4), 345–355.

39. Ji, Y., et al., Mouse embryo fibroblasts lacking the tumor suppressor menin show altered expression of extracellular matrix protein genes. Mol Cancer Res, 2007. 5(10): p. 1041-51.

40. Juhaszova, M., & Blaustein, M. P. (1997). Na+pump low and high ouabain affinity α subunit isoforms are differently distributed in cells. Proceedings of the National Academy of Sciences of the United States of America, 94(5), 1800–1805.

41. Gosmanov, A.R., E.G. Schneider, and D.B. Thomason, NKCC activity restores muscle water during hyperosmotic challenge independent of insulin, ERK, and p38 MAPK. Am J Physiol Regul Integr Comp Physiol, 2003. 284(3): p. R655-65.

42. Zhao, H., R. Hyde, and H.S. Hundal, Signaling mechanisms underlying the rapid and additive stimulation of NKCC activity by insulin and hypertonicity in rat L6 skeletal muscle cells. J Physiol, 2004. 560(Pt 1): p. 123-36.

43. Shen, M.R., et al., Insulin-like growth factor 1 stimulates KCl cotransport, which is necessary for invasion and proliferation of cervical cancer and ovarian cancer cells. J Biol Chem, 2004. 279(38): p. 40017-25.

44. Hay, N. and N. Sonenberg, Upstream and downstream of mTOR. Genes Dev, 2004. 18(16): p. 1926-45.

45. Dennis, P.B., Jaeschke, A., Saitoh, M., Fowler, B., Kozma, S.C., and Thomas, G. 2001. Mammalian TOR: A homeostatic ATP sensor. Science 294: 1102–1105.

46. Hardie, D.G., Carling, D., and Carlson, M. 1998. The AMP activated/SNF1 protein kinase subfamily: Metabolic sensors of the eukaryotic cell? Annu. Rev. Biochem. 67: 821–855.

47. Kemp, B.E., Mitchelhill, K.I., Stapleton, D., Michell, B.J., Chen, Z.P., and Witters, L.A. 1999. Dealing with energy demand: The AMP-activated protein kinase. Trends Biochem. Sci. 24: 22–25.

48. Christian Lytle1, Thomas J. McManus2, and Mark Haas2. A model of Na-K-2Cl cotransport based on ordered ion binding and glide symmetry. Vol. 274 no. 2, C299-C309 DOI.

49. P. K. Lauf, J. Bauer, N. C. Adragna, H. Fujise, A. M. Zade-Oppen, K. H. Ryu, E. Delpire. Erythrocyte K-Cl cotransport: properties and regulation. Vol. 263 no. 5, C917-C932 DOI.

50. Bayeva, M., et al., mTOR regulates cellular iron homeostasis through tristetraprolin. Cell Metab, 2012. 16(5): p. 645-57.

51. Veland, I.R., et al., Inversin/Nephrocystin-2 is required for fibroblast polarity and directional cell migration. PLoS One, 2013. 8(4): p. e60193.

52. Greenough, M.A., et al., Presenilins promote the cellular uptake of copper and zinc and maintain copper chaperone of SOD1-dependent copper/zinc superoxide dismutase activity. J Biol Chem, 2011. 286(11): p. 9776-86.

53. Ewalt, D.H., et al., Renal lesion growth in children with tuberous sclerosis complex. J Urol, 1998. 160(1): p. 141-5.

54. Sancak, O., et al., Mutational analysis of the TSC1 and TSC2 genes in a diagnostic setting: genotype--phenotype correlations and comparison of diagnostic DNA techniques in Tuberous Sclerosis Complex. Eur J Hum Genet, 2005. 13(6): p. 731-41.

55. Jones, A.C., et al., Comprehensive mutation analysis of TSC1 and TSC2-and phenotypic correlations in 150 families with tuberous sclerosis. Am J Hum Genet, 1999. 64(5): p. 1305-15.

56. Van Slegtenhorst, M., et al., Mutational spectrum of the TSC1 gene in a cohort of 225 tuberous sclerosis complex patients: no evidence for genotype-phenotype correlation. J Med Genet, 1999. 36(4): p. 285-9.

57. Kockskamper, J., G. Gisselmann, and H.G. Glitsch, Comparison of ouabain-sensitive and -insensitive Na/K pumps in HEK293 cells. Biochim Biophys Acta, 1997. 1325(2): p. 197-208.

58. Nguyen, A.N., D.P. Wallace, and G. Blanco, Ouabain binds with high affinity to the Na,K-ATPase in human polycystic kidney cells and induces extracellular signal-regulated kinase activation and cell proliferation. J Am Soc Nephrol, 2007. 18(1): p. 46-57.

59. Benade, L.E., et al., Ouabain sensitivity is linked to ras -transformation in human HOS cells. Biochem Biophys Res Commun, 1986. 136(2): p. 807-14.

60. Beck, J., et al., Na-K-Cl cotransporter contributes to glutamate-mediated excitotoxicity. J Neurosci, 2003. 23(12): p. 5061-8.

61. Canessa, M., et al., Volume-stimulated, Cl(-)-dependent K+ efflux is highly expressed in young human red cells containing normal hemoglobin or HbS. J Membr Biol, 1987. 97(2): p. 97-105.

62. Quarmyne, M.O., et al., Volume regulation and KCl cotransport in reticulocyte populations of sickle and normal red blood cells. Blood Cells Mol Dis, 2011. 47(2): p. 95-9.

63. Lauf, P.K. and B.E. Theg, A chloride dependent K+ flux induced by N-ethylmaleimide in genetically low K+ sheep and goat erythrocytes. Biochem Biophys Res Commun, 1980. 92(4): p. 1422-8.

64. Dunham, P.B., G.W. Stewart, and J.C. Ellory, Chloride-activated passive potassium transport in human erythrocytes. Proc Natl Acad Sci U S A, 1980. 77(3): p. 1711-5.

65. Adragna, N.C., M. Di Fulvio, and P.K. Lauf, Regulation of K-Cl cotransport: from function to genes. J Membr Biol, 2004. 201(3): p. 109-37.

66. Roberto Antolovic. Low nanomolar concentrations of ouabain may induce higher activity of the Na+/K+-ATPase in human erythrocytes. Veterinarski Arhiv 76 (6), 489-495, 2006.